



**HAL**  
open science

## **Impact of the Fukushima accident on tritium, radiocarbon and radiocesium levels in seawater of the western North Pacific Ocean: A comparison with pre-Fukushima situation**

Pavel P. Povinec, Laval Liong Wee Kwong, Jakub Kaizer, M. Molnar, Hartmut Nies, L. Palcsu, Laszlo Papp, Mia Khanh Pham, P. Jean-Baptiste

### ► To cite this version:

Pavel P. Povinec, Laval Liong Wee Kwong, Jakub Kaizer, M. Molnar, Hartmut Nies, et al.. Impact of the Fukushima accident on tritium, radiocarbon and radiocesium levels in seawater of the western North Pacific Ocean: A comparison with pre-Fukushima situation. *Journal of Environmental Radioactivity*, 2017, 166 (Part 1), pp.56-66. 10.1016/j.jenvrad.2016.02.027 . hal-01584220

**HAL Id: hal-01584220**

**<https://hal.science/hal-01584220v1>**

Submitted on 24 Jun 2021

**HAL** is a multi-disciplinary open access archive for the deposit and dissemination of scientific research documents, whether they are published or not. The documents may come from teaching and research institutions in France or abroad, or from public or private research centers.

L'archive ouverte pluridisciplinaire **HAL**, est destinée au dépôt et à la diffusion de documents scientifiques de niveau recherche, publiés ou non, émanant des établissements d'enseignement et de recherche français ou étrangers, des laboratoires publics ou privés.

## **Impact of the Fukushima accident on tritium, radiocarbon and radiocesium levels in seawater of the western North Pacific Ocean: a comparison with pre-Fukushima situation**

**ABSTRACT:** Tritium, radiocarbon and radiocesium concentrations in water column samples in coastal waters offshore Fukushima and in the western North Pacific Ocean collected in 2011-2012 during the Ka'imikai-o-Kanaloa (KoK) cruise are compared with other published results. The highest levels in surface seawater were observed for  $^{134}\text{Cs}$  and  $^{137}\text{Cs}$  in seawater samples collected offshore Fukushima (up to  $1.1 \text{ Bq L}^{-1}$ ), which represent an increase by about three orders of magnitude when compared with the pre-Fukushima concentration. Tritium levels were much lower (up to  $0.15 \text{ Bq L}^{-1}$ ), representing an increase by about a factor of 6. The impact on the radiocarbon distribution was measurable, but the observed levels were only by about 9% above the global fallout background. The  $^{137}\text{Cs}$  (and similarly  $^{134}\text{Cs}$ ) inventory in the water column of the investigated western North Pacific region was  $(2.7 \pm 0.4) \text{ PBq}$ , while for  $^3\text{H}$  it was only  $(0.3 \pm 0.2) \text{ PBq}$ . Direct releases of highly contaminated water from the damaged Fukushima NPP, as well as dry and wet depositions of these radionuclides over the western North Pacific considerably changed their distribution patterns in seawater. Presently we can distinguish Fukushima labeled waters from global fallout background thanks to short-lived  $^{134}\text{Cs}$ . However, in the long-term perspective when  $^{134}\text{Cs}$  will decay, new distribution patterns of  $^3\text{H}$ ,  $^{14}\text{C}$  and  $^{137}\text{Cs}$  in the Pacific Ocean should be established for future oceanographic and climate change studies in the Pacific Ocean.

*Keywords:* Fukushima accident; radionuclides in seawater; KoK cruise; GEOSECS; WOCE; WOMARS

<http://www.elsevier.com/open-access/userlicense/1.0/>

## 37 1. Introduction

38

39 Large quantities of radionuclides were released during the Fukushima Dai-ichi Nuclear Power  
40 Plant (NPP) accident (starting on 11 March 2011) to the atmosphere (Chino et al., 2011;  
41 Hirose, 2012) and to coastal waters (Kawamura et al., 2011; Povinec et al., 2013a; Aoyama et  
42 al. 2015a, b). From a radiological point of view,  $^{137}\text{Cs}$  has been considered to be the most  
43 important anthropogenic radionuclide in the environment because of its large releases,  
44 relatively long half-life, and its relative high bioavailability. Due to its accumulation in  
45 tissues, it has been relevant for delivering radiation doses to the public from the consumption  
46 of food (Aarkrog et al., 1997; Livingston and Povinec, 2000). Another radioecologically  
47 important radionuclide, which may be released in large quantities during nuclear accidents is  
48  $^{131}\text{I}$ , however, because of its short half-life (8.02 days), its contribution is dominant to  
49 terrestrial radiation doses during first days after the accident (Povinec et al., 2013a).

50 About 15—20 PBq of radiocesium (for  $^{134}\text{Cs}$  and  $^{137}\text{Cs}$  each) was released during the  
51 Fukushima accident to the atmosphere (Chino et al., 2011; Povinec et al., 2013a, b; Aoyama  
52 et al. 2015a), which occurred mainly between 12 and 16 March, with smaller contributions up  
53 to March 24. Most of the radionuclides released to the atmosphere were rapidly associated  
54 with aerosols, representing a major form of pollutants in the atmosphere, which have been  
55 then distributed globally (Masson et al., 2011; Povinec et al., 2013a, b). The radionuclides  
56 moved with the prevailing western winds mainly from Fukushima over the Pacific Ocean  
57 (Povinec et al., 2013c), with only a partial contamination of the Japanese land (Hirose, 2012)  
58 and the Japan Sea (Inoue et al., 2012).

59 After passing the Pacific Ocean, North America, the Atlantic Ocean, and Europe, the  
60 radioactive clouds went back across the Asian continent. At the beginning of April 2011, the  
61 northern hemisphere was labeled with Fukushima-derived radionuclides (Masson et al., 2011;  
62 Hernández-Ceballos et al., 2012; Povinec et al., 2013a, b). The aerosols with captured  
63 radionuclides were then deposited on the Earth's surface including the ocean by wet and dry  
64 deposition. About 80 % was deposited over the North Pacific Ocean, about 20 % over Japan,  
65 and less than 2% over the Atlantic and Europe (Morino et al., 2011; Stohl et al., 2012;  
66 Yoshida and Kanda, 2012).

67 We shall discuss in this paper radionuclide variations in the water column of the western  
68 North Pacific Ocean after the Fukushima accident. Distribution of several radionuclides  
69 dissolved in seawater (e.g.,  $^3\text{H}$ ,  $^{90}\text{Sr}$ ,  $^{129}\text{I}$ ,  $^{134}\text{Cs}$ ,  $^{137}\text{Cs}$ ) has already been under investigations  
70 (e.g., Aoyama et al., 2012, 2013, 2015a; Buesseler et al., 2012; Hou et al. 2013; Povinec et

71 al., 2012, 2013a, d). We shall focus in this paper on Fukushima impact on  $^3\text{H}$ ,  $^{14}\text{C}$  and  
72 radiocesium levels in water column of the western North Pacific Ocean.

73 Cesium radioisotopes, namely  $^{137}\text{Cs}$  (half-life  $T_{1/2} = 30.17$  yr) and  $^{134}\text{Cs}$  ( $T_{1/2} = 2.06$  yr)  
74 have been the most frequently studied radionuclides in seawater after the Fukushima accident.  
75 Presence of  $^{134}\text{Cs}$  in seawater clearly indicates its Fukushima origin as because of the short  
76 half-life  $^{134}\text{Cs}$  from global fallout and the 1986 Chernobyl accident has already decayed. The  
77 nuclear accident at the Fukushima Dai-ichi NPP increased  $^{137}\text{Cs}$  concentrations in coastal  
78 seawater in March 2011 up to  $68 \text{ kBq L}^{-1}$ , eight orders of magnitude above the global fallout  
79 background (Povinec et al., 2013a; Povinec and Hirose, 2015). This increase was due to direct  
80 liquid releases of  $^{137}\text{Cs}$  contaminated fresh and later also seawater to coastal waters, which  
81 was estimated to be around 4 PBq (Kawamura et al., 2011; Tsumune et al., 2012, 2013;  
82 Aoyama et al., 2016a, b). The  $^{131}\text{I}/^{137}\text{Cs}$  activity ratio in surface seawater offshore Fukushima  
83 indicated that most of the radiocesium observed in coastal waters was the result of a direct  
84 discharge to the ocean (Hou et al., 2013). Due to the transport of water masses from the  
85 Japanese coast to the open western North Pacific by the coastal currents (Nakano and  
86 Povinec, 2003, 2012; Tsumune et al., 2012, 2013), the high  $^{137}\text{Cs}$  concentrations observed in  
87 2011 in coastal seawater decreased rapidly with apparent half-life of about 1 year (Povinec  
88 and Hirose, 2015). The typical  $^{137}\text{Cs}$  activity concentrations in coastal waters in 2011-2012  
89 were from a few  $\text{mBq L}^{-1}$  to a few  $\text{Bq L}^{-1}$  (Aoyama et al., 2012, 2013; Buesseler et al., 2012;  
90 Honda et al., 2012; Povinec et al. 2013a, d; Kameník et al., 2013; Kumamoto et al., 2013a).

91 Only a little attention has been given till now to tritium (Povinec et al., 2013a, d;  
92 Matsumoto et al., 2013; Steinhauser, 2014), mainly because of the fact that liquid tritium  
93 releases when compared with radiocesium were much lower (0.1-0.5 PBq; Povinec et al.,  
94 2013d). Radiological impact due to tritium is low because of its short physical half-life (12.32  
95 y), its short effective biological half-life in the human body (10 days, Kim et al., 2011), the  
96 low energy of emitted beta-decay electrons (18.6 keV) and its low production rates in nuclear  
97 reactors (Chudý and Povinec, 1982; Povinec et al., 2013a).

98 Similarly a radiological impact of radiocarbon on the marine environment and on humans  
99 has been expected to be low due to its low production rates in nuclear reactors (Chudý and  
100 Povinec, 1982). When compared with the Chernobyl accident, where due to  $^{14}\text{C}$  production in  
101 the graphite moderator in the  $^{13}\text{C}(n, \gamma)^{14}\text{C}$  reaction, and the graphite burning during the  
102 accident, the  $^{14}\text{C}$  release to the atmosphere was estimated to be around 44 TBq (Povinec et al.,  
103 2013a). Elevated  $^{14}\text{C}$  levels (up to 124 pMC (% Modern Carbon) or  $281.6 \text{ Bq kg}^{-1}$  of carbon)  
104 were measured in tree rings collected about 2.5 km from the Chernobyl NPP (Buzinny et al.

105 1998). However, the  $^{14}\text{C}$  effect was not measurable in Central Europe (Povinec et al., 1988).  
106 There are no data available on radiocarbon in the atmosphere or in seawater after the  
107 Fukushima accident.

108 The aim of the present study has been to assess, compare and evaluate tritium, radiocarbon  
109 and radiocesium records in the water column of the western North Pacific Ocean after the  
110 Fukushima accident. It has been important to estimate changes in  $^3\text{H}$ ,  $^{14}\text{C}$  and  $^{137}\text{Cs}$   
111 concentrations in Pacific waters after the Fukushima accident not only from a radioecological  
112 point of view, but also due to the fact that these radionuclides have been frequently used as  
113 tracers of ocean and ocean-atmosphere processes. We need to know how radionuclide  
114 concentrations have changed in the Pacific Ocean after the Fukushima accident, and how we  
115 can apply pre-Fukushima and post-Fukushima data in oceanographic research. The observed  
116 radionuclide patterns and their comparison with pre-Fukushima data will contribute to future  
117 oceanographic and climate studies using these radionuclides as tracers of processes in the  
118 marine environment.

119 The radionuclide data presented in this paper were obtained from analyses of seawater  
120 samples collected during the KoK (Ka'imikai-o-Kanaloa) cruise, carried out in June 2011  
121 offshore Fukushima. Preliminary data on tritium and radiocesium (mostly surface samples)  
122 were discussed in our previous paper (Povinec et al., 2013d). In the present paper we discuss  
123 the final data set on tritium (21 results) and radiocesium (45 results), together with 12  
124 radiocarbon results (Table 1). A comprehensive radiocesium data set, covering the KoK  
125 seawater sampling, has been published by Buesseler et al. (2012). In this paper we report  
126 complementary  $^3\text{H}$ ,  $^{14}\text{C}$ ,  $^{134}\text{Cs}$  and  $^{137}\text{Cs}$  data, and compare them with recently published post-  
127 Fukushima radiocesium data (Aoyama et al., 2012a,b; 2013; 2015a, b; Buesseler et al., 2012;  
128 Kaeriyama et al., 2013; Kumamoto et al., 2013a, 2014, 2015), as well as with pre-Fukushima  
129  $^3\text{H}$ ,  $^{14}\text{C}$  and  $^{137}\text{Cs}$  data obtained for the western North Pacific Ocean (Ostlund et al., 1987;  
130 Watanabe et al., 1991; Tsunogai et al., 1995; Aramaki et al., 2001; Kumamoto et al., 2002;  
131 Povinec et al. 2003, 2004c, 2010).

132

## 133 **2. Direct releases and atmospheric deposition of $^{137}\text{Cs}$ , $^3\text{H}$ and $^{14}\text{C}$ during the Fukushima** 134 **accident to the western North Pacific Ocean**

135135

### 136 *2.1. Radiocesium*

137137

138 The largest radionuclide releases to the coastal ocean were due  $^{137}\text{Cs}$  because of its large  
139 production rates in the damaged Fukushima nuclear reactors (yield 6.2%). The  $^{137}\text{Cs}$   
140 inventory in the damaged nuclear reactors has been estimated to be about 700 PBq (230 PBq  
141 recovered), and 140 PBq in stagnant water (Povinec et al., 2013a). The  $^{134}\text{Cs}$  production in the  
142 damaged Fukushima nuclear reactors was similar to that of  $^{137}\text{Cs}$ , therefore its inventory and  
143 the direct  $^{134}\text{Cs}$  releases to the sea were estimated to be similar to  $^{137}\text{Cs}$  ones on the basis of  
144 their activity ratio close to one (Kirchner et al., 2012).

145145

#### 146 *2.1.1. Direct releases of radiocesium to the sea*

147147

148 Kawamura et al. (2011) using the TEPCO (Tokyo Electric Power Company) data and  
149 numerical simulations estimated the total  $^{137}\text{Cs}$  release for the period from 21 March to 30  
150 April 2011 to be 4 PBq. Tsumune et al. (2013) using a global ocean circulation model and the  
151 available  $^{137}\text{Cs}$  monitoring data estimated the direct  $^{137}\text{Cs}$  releases between 26 March and 31  
152 May 2011 to be  $3.5 \pm 0.7$  PBq. Similar estimations were obtained using various oceanic  
153 models: 1-3.5 PBq by Dietze and Kriest (2012), 4.1-4.5 PBq by Estournel et al. (2012), and  
154 5.5–5.9 PBq by Miyazawa et al. (2012a, b). Recently Aoyama et al. (2015a, b) critically  
155 reviewed the different  $^{137}\text{Cs}$  release rate scenarios, and their best estimation is  $3.6 \pm 0.7$  PBq.

156156

#### 157 *2.1.2. Deposition of radiocesium over the Pacific Ocean*

158158

159 The estimation of the atmospheric deposition of  $^{137}\text{Cs}$  over the Pacific Ocean is even more  
160 difficult task in the evaluation of its source term in the ocean (Kawamura et al., 2011; Morino  
161 et al., 2011; Buessler et al., 2012; Stohl et al., 2012; Honda et al., 2012; Rypina et al., 2013).  
162 Dietze and Kriest (2012) estimated the accumulated atmospheric deposition of  $^{137}\text{Cs}$  in the  
163 range of 50 — 200 kBq m<sup>-2</sup>. It has been expected therefore that the wet and dry deposition  
164 over the huge Pacific Ocean may dominate over the radiocesium transport from coastal waters  
165 to the open ocean (Aoyama et al., 2015a, b). Rypina et al. (2013) using the KoK data  
166 estimated the contribution from the atmospheric source to be in the range of 0 – 11 PBq. The  
167 KoK data are, however, not well-suited for constraining the atmospheric source strength  
168 because of the restricted sampling area (only about 600 km east from the coast), and the fact  
169 that most of the Fukushima fallout  $^{137}\text{Cs}$  had left the survey area by mid-June when the KoK  
170 sampling cruise was carried out. Aoyama et al. (2015b) recently reviewed the available data

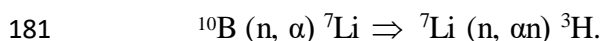
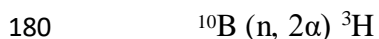
171 and came with the estimation that the  $^{137}\text{Cs}$  wet and dry deposition over the North Pacific  
172 Ocean should be in the range of 12-15 PBq from the total atmospheric release of 14-17 PBq.

173173

## 174 2.2. Tritium

175175

176 Tritium production in the Fukushima boiling-water reactors was mainly due to a ternary  
177 fission of  $^{235}\text{U}$  (yield of 0.013%) and of  $^{239}\text{Pu}$  (0.023%), with the estimated annual  $^3\text{H}$   
178 production of about 1 PBq/GW<sub>e</sub> (Povinec et al., 2013a). Tritium was also produced in nuclear  
179 reactions with  $^{10}\text{B}$  in boron carbide control rods



182 Further, the  $^3\text{H}$  production was also due to the neutron capture reaction on deuterium present  
183 in the water coolant ( $^2\text{H} (n, \gamma) ^3\text{H}$ ) and in the reaction  $^7\text{Li} (n, \alpha n) ^3\text{H}$  on lithium impurities in  
184 the water. The nuclear reaction contributions to the annual  $^3\text{H}$  production were, however,  
185 much smaller (about 0.1 TBq/GW<sub>e</sub>) than the ternary fission. Tritium will not be released at  
186 once even if the fuel and the boron control rods would be damaged. Generally, boiling-water  
187 nuclear reactors produce less tritium than pressurized water reactors and much less than heavy  
188 water reactors (Chudý and Povinec, 1982; Povinec et al., 2013a).

189 The  $^3\text{H}$  inventory in three damaged nuclear reactors was estimated to be about 3.4 PBq (1-  
190 1.2 PBq in each reactor; Nishihara et al., 2012; [http://www.meti.go.jp/earthquake/  
191 nuclear/pdf/140424/140424\\_02\\_008.pdf](http://www.meti.go.jp/earthquake/nuclear/pdf/140424/140424_02_008.pdf)), much higher than the value of 0.018 PBq reported  
192 by Schwantes et al. (2012). From the total of 3.4 PBq produced tritium, about 0.8 PBq was  
193 stored in tanks, about 0.05 PBq was in stagnant water accumulated in the reactors and  
194 turbines buildings, and about 0.05 PBq was in seawater pipe trenches. Rest of the tritium  
195 inventory should be in the fuel debris, and part of it was released directly to the sea.

196 The  $^3\text{H}$  activity concentration in stagnant water in June 2011 was in the range 0.7–20 MBq  
197 L<sup>-1</sup> (lower by a factor of about 10<sup>5</sup> when compared e.g. with heavy water reactors). The  
198 release ratio from nuclear cores to the stagnant water was estimated to be the highest for  $^3\text{H}$   
199 (46%),  $^{131}\text{I}$  (32%), and  $^{137}\text{Cs}$  (20%), but only 1.6% for  $^{90}\text{Sr}$  (Nishihara et al., 2012). This  
200 would indicate that the maximal direct releases to the sea could be for  $^{131}\text{I}$ ,  $^{137}\text{Cs}$ ,  $^{90}\text{Sr}$  and  $^3\text{H}$ ,  
201 of about 1900, 140, 8 PBq and 1.6, respectively (if all the stagnant water would be released to  
202 the sea). The  $^3\text{H}/^{137}\text{Cs}$  and  $^3\text{H}/^{90}\text{Sr}$  activity ratios in the stagnant water were  $7 \times 10^{-3}$  and 0.2,  
203 respectively, which could be expected in coastal waters as well. Additionally, during the



204 accident, external cooling with fresh and later also with seawater was carried out, which could  
205 also increase radionuclide levels in coastal waters.

206 At present the total water volume in storage tanks at the Fukushima NPP site is about  
207 460,000 m<sup>3</sup>, which is undergoing decontamination (except for tritium) in a Multi-Nuclide  
208 Removal System (ALPS), with typical <sup>3</sup>H activity concentrations of 800 kBq L<sup>-1</sup> (Povinec et  
209 al., 2013a). It is very likely that the tritiated water will be discharged to the sea, or evaporated  
210 and released to the atmosphere.

211 Unfortunately, there are no data available on tritium levels during the early stage of the  
212 Fukushima NPP accident at the seaport, close to discharge points. The TEPCO reported for  
213 August 2013 a value of 68 Bq L<sup>-1</sup> ([www.TEPCO.com](http://www.TEPCO.com)). We shall estimate the total amount of  
214 <sup>3</sup>H released to coastal waters and deposited over the North Pacific Ocean later when we shall  
215 calculate both the <sup>137</sup>Cs and <sup>3</sup>H inventories in the water column. A preliminary estimation of  
216 the total <sup>3</sup>H releases to the marine environment (using a very limited data set) was in the range  
217 of 0.1-0.5 PBq (Povinec et al., 2013d). Estimation of the <sup>3</sup>H source term in the western North  
218 Pacific Ocean depends strongly on the estimations of direct liquid releases and atmospheric  
219 depositions of <sup>137</sup>Cs on the studied sea areas. Therefore with improving our knowledge of the  
220 <sup>137</sup>Cs source term, the estimation of the <sup>3</sup>H source term will also improve.

221 Generally, the tritium inventory should be much smaller when compared with global  
222 fallout and with natural production of tritium. The total bomb produced tritium inventory was  
223 estimated to be around 186 EBq in the atmosphere and 113 EBq in the ocean, from which 8  
224 EBq was still present in 2010 (Povinec et al., 2010, 2013a). The inventory of <sup>3</sup>H discharged  
225 from reprocessing nuclear facilities to the ocean was 410 PBq, from which 45 PBq was still  
226 present in 2010. The annual cosmic-ray production, predominantly in the reactions

227  $^{14}\text{N} (n, ^3\text{H}) ^{12}\text{C}$  and  $^{16}\text{O} (n, ^3\text{H}) ^{14}\text{N}$

228 is much lower, around 0.15 EBq, varying with cosmic-ray flux. The world steady-state natural  
229 inventory is about 2.2 EBq.

230230

### 231 2.3. Radiocarbon

232232

233 There are no data available on radiocarbon source term, and on its gaseous and liquid releases  
234 after the Fukushima accident. Radiocarbon is an activation product formed mainly in the <sup>14</sup>N  
235 (n, p) <sup>14</sup>C and <sup>17</sup>O (n, α) <sup>14</sup>C nuclear reactions on target nuclei present in the fuel, and on  
236 impurities in the fuel rods and in the coolant/moderator (Chudý and Povinec, 1982). The <sup>14</sup>C  
237 is also produced in ternary fission (with yield of 1.6 × 10<sup>-4</sup> %), however, its contribution is

238 negligible when compared with nuclear reactions. For the BWR reactors the dominant annual  
239 production is on  $^{14}\text{N}$  impurities in the fuel, in the rods and in the water coolant (1.3 TBq/GW<sub>e</sub>)  
240 and on  $^{17}\text{O}$  present in the fuel and in the water coolant (0.7 TBq/GW<sub>e</sub>). The total annual  $^{14}\text{C}$   
241 production in BWRs is estimated to be around 2 TBq/GW<sub>e</sub>, from which about 1.2 TBq/GW<sub>e</sub>  
242 should be present in the fuel rods, and about 0.8 TBq/GW<sub>e</sub> in the water coolant (Povinec et  
243 al., 2013a).

244 Generally, the production rates of Fukushima-derived radiocarbon should be negligible  
245 when compared with bomb produced radiocarbon, and its natural production by cosmic rays.  
246 The radiocarbon inventory due to atmospheric nuclear bomb tests was about 213 PBq in the  
247 atmosphere and about 130 PBq in the ocean (UNSCEAR, 2008). The  $^{14}\text{C}$  inventory from  
248 discharges from reprocessing nuclear facilities was about 2 PBq, mostly in the marine  
249 environment (Povinec et al., 2000). The natural  $^{14}\text{C}$  is produced in the atmosphere by cosmic-  
250 ray neutrons in the same reactions as mentioned above, the dominant reaction being  $^{14}\text{N}(\text{n}, \text{p})$   
251  $^{14}\text{C}$ . The annual  $^{14}\text{C}$  production is about 1.4 PBq, which vary with the cosmic-ray flux. The  
252 total inventory is about 8.5 EBq, of which about 0.14 EBq is in the atmosphere and rest is  
253 mostly in oceans (UNSCEAR, 2008).

254254

### 255 **3. Samples and methods**

256256

#### 257 *3.1. Seawater samples*

258258

259 Seawater samples were collected offshore Fukushima during the US expedition using the  
260 research vessel Ka'imikai-o-Kanaloa (KoK) of the University of Hawaii (3—17 June, 2011)  
261 from about 30 km to about 600 km (from 34 to 38° N, and from 141.5 to 147° E) east of the  
262 Japan coast (Buesseler et al., 2012). Locations of KoK sampling stations used in this study are  
263 shown in Fig. 1a. Water column sampling stations, visited during other cruises (which have  
264 been used for comparison) are shown in Fig. 1b.

265 Surface samples for radionuclide analyses were collected using a water pump. Water  
266 column samples were collected at different depths using a Rosette sampling system equipped  
267 with Niskin bottles. Half liter of seawater was used both for  $^3\text{H}$  and  $^{14}\text{C}$  analyses, while  $^{137}\text{Cs}$   
268 was analyzed in 1 L seawater samples. The bottles had double plugs to prevent a penetration  
269 of air into the water sample during transport and storage. Surface seawater samples were  
270 collected at 17 stations, and water profile samples at 12 stations.

271271

272 2.2. Tritium analysis

273273

274 Pre-screening of  $^3\text{H}$  levels in seawater samples (to avoid possible contamination) was carried  
275 out in the Bratislava laboratory by direct  $^3\text{H}$  counting (after triple distillation) in water-liquid  
276 scintillator cocktails using Packard liquid scintillation spectrometer. Tritium was then  
277 precisely analyzed in seawater samples in the Debrecen and Saclay laboratories using the  $^3\text{He}$   
278 in-growth mass spectrometry method. The procedure used in Debrecen (Palcsu et al., 2010)  
279 consists of three major steps: First, the water sample is put into a stainless steel vessel, and the  
280 dissolved gases including helium are removed from the water by vacuum pumping. The  
281 samples are then stored for several months so that  $^3\text{He}$  atoms are produced by tritium decay.  
282 The helium fraction is finally admitted to a dual collector noble gas mass spectrometer, where  
283 the abundance of the tritiogenic  $^3\text{He}$  is measured, and  $^3\text{H}$  activity is calculated.

284 In the procedure used in Saclay (Jean-Baptiste et al., 2010) the water samples were  
285 transferred and sealed in low helium diffusivity glass bulbs that had been previously baked at  
286  $600^\circ\text{C}$  under a stream of argon. After an equilibrium time of about 100-150 days, the bulbs  
287 were then connected to a MAP-215-50 noble gas mass spectrometer equipped with a stainless  
288 steel low blank inlet system ( $^3\text{He}$  blank  $< 3 \times 10^{-20}$  mol) for measurements that were calibrated  
289 against an air standard ( $\text{He} = 5.24$  ppm,  $^3\text{He}/^4\text{He} = 1.38 \times 10^{-6}$ ) drawn from a 5 L tank filled  
290 with clean air at known pressure, temperature and relative humidity conditions, through a  
291 precisely calibrated volume of  $122.2 \pm 0.1$  (at 2 sigma)  $\text{mm}^3$ . The  $^3\text{He}$  ingrowth method can  
292 measure  $^3\text{H}$  levels down to 0.01 TU (precision at  $1 \sigma$  is around 0.005 TU).

293 It has been widely accepted in oceanographic studies that tritium levels has been reported  
294 in Tritium Units (TU). One TU represents an isotope ratio of 1  $^3\text{H}$  atom to  $10^{18}$  protium ( $^1\text{H}$ )  
295 atoms, which is equivalent to  $0.118 \text{ Bq L}^{-1}$  of water.

296296

297 2.3. Radiocarbon analysis

298298

299 The  $^{14}\text{C}$  measurements from dissolved inorganic carbon (DIC) of the seawater samples were  
300 carried out using an accelerator mass spectrometry (AMS) in the Debrecen laboratory.  
301 However, to avoid a possible  $^{14}\text{C}$  contamination of the AMS system, a few seawater samples  
302 with highest  $^{137}\text{Cs}$  levels were checked for  $^{14}\text{C}$  content in the Bratislava laboratory by a gas  
303 proportional counting technique (Povinec et al., 2013e). For AMS analyses, the dissolved  
304  $\text{CO}_2$  was extracted from 20 mL seawater samples by adding 85% phosphoric acid, followed  
305 by 2 hours heating at  $75^\circ\text{C}$  in a heating block. The degassed  $\text{CO}_2$  was extracted and

306 cryogenically cleaned in a vacuum line (Molnár et al., 2013a). The obtained pure CO<sub>2</sub> gas  
307 was then converted to graphite by sealed tube graphitization method (Rinyu et al., 2013). The  
308 <sup>14</sup>C measurements from the graphite targets were performed with a MICADAS type AMS in  
309 the Debrecen laboratory (Molnár et al., 2013b). The overall measurement uncertainty for each  
310 sample was below 5‰, including normalization, background subtraction, and counting  
311 statistics. The <sup>14</sup>C results were corrected for decay of the standard and for isotope  
312 fractionation using <sup>13</sup>C measurements.

313 The <sup>14</sup>C concentration is given as Δ<sup>14</sup>C (in ‰), relative to the NIST (National Institute of  
314 Standards and Technology, Gaithersburg, USA) <sup>14</sup>C oxalic acid standard (Stuiver and  
315 Ostlund, 1983)

$$316 \quad \Delta^{14}\text{C} = \delta^{14}\text{C} - 2(\delta^{13}\text{C} + 25)(1 + \delta^{14}\text{C}/1000) (\text{‰}) \quad (\text{eq. 1})$$

$$317 \quad \delta^{14}\text{C} = \delta^{14}\text{C} = [({}^{14}\text{C}_{\text{sample}} - {}^{14}\text{C}_{\text{standard}})/{}^{14}\text{C}_{\text{standard}}] \times 1000 (\text{‰}) \quad (\text{eq. 2})$$

318 The δ<sup>13</sup>C is the <sup>13</sup>C/<sup>12</sup>C ratio measured by the AMS simultaneously with the <sup>14</sup>C measurement.

319319

## 320 2.4. Analysis of radiocesium

321321

322 The seawater samples were nondestructively counted directly using high efficiency HPGe  
323 spectrometers placed in the in the CAVE (Counting Laboratory for Environmental  
324 Radionuclides) underground facility of IAEA-EL (Povinec et al., 2004a, b, 2005b, 2012b).  
325 The counting periods were between 24 and 72 hours.

326 The data quality of radionuclide analyses was assured by regular participation in  
327 intercomparison exercises, and by analysis of IAEA (International Atomic Energy Agency)  
328 reference materials (Irish Sea water: IAEA-381, Povinec et al., 2002; Mediterranean Sea  
329 water: IAEA-418, Pham et al., 2010; and Irish Sea water: IAEA-443, Pham et al., 2011).

330330

## 331 4. Results and discussion

332332

### 333 4.1 Radiocesium

334334

335 The measured <sup>137</sup>Cs activity concentrations in surface waters collected 30-600 km offshore  
336 the Fukushima NPP ranged from 15 mBq L<sup>-1</sup> to 1120 mBq L<sup>-1</sup> (Table 1, Fig. 2a). They were  
337 by about three orders of magnitude higher than the global fallout background, although the  
338 cruise track did not go closer than 30 km from the coast. Even at distances around 600 km off  
339 Fukushima, <sup>137</sup>Cs activity concentrations of around 0.2 Bq L<sup>-1</sup> were found, i.e. by about a

340 factor of 200 above the global fallout background of 1 mBq L<sup>-1</sup>. The observed elevated <sup>137</sup>Cs  
341 levels covered an area of around 150 000 km<sup>2</sup> (south of 38° N and west of 147° E).

342 A considerable decrease in surface <sup>137</sup>Cs levels took place between the KoK cruise  
343 measurements (3.5 Bq L<sup>-1</sup>, June 2011) and those carried out earlier when about 24 Bq L<sup>-1</sup> of  
344 <sup>137</sup>Cs were measured in seawater 30 km offshore Fukushima (Povinec et al., 2013a). The  
345 <sup>134</sup>Cs and <sup>137</sup>Cs data presented in Table 1 confirms that the <sup>134</sup>Cs/<sup>137</sup>Cs activity ratio in the  
346 analyzed seawater samples was close to 1, clearly indicating that the source of these  
347 radionuclides was the Fukushima accident.

348 Figure 2a clearly separates the western KoK stations with higher <sup>137</sup>Cs levels from the  
349 eastern stations with smaller activity concentrations. The geographical distribution of <sup>137</sup>Cs  
350 levels in the water column indicates that an atmospheric deposition of <sup>137</sup>Cs occurred within  
351 the 600 km zone offshore Fukushima. For example, the increased <sup>3</sup>H, <sup>134</sup>Cs and <sup>137</sup>Cs  
352 activities found at St. 8 (Table 1), in agreement with other KoK data (Buesseler et al., 2012),  
353 should not be affected by direct liquid releases from the Fukushima NPP, but an atmospheric  
354 deposition took place there.

355 At some stations (e.g., St. 18, 24) subsurface maxima at 50 m water depth have already been  
356 observed three months after the accident (Table 1, Fig. 2a). At other stations (e.g., St. 22, 25  
357 and 26) located closer to the Fukushima coast, the maximum radiocesium levels were  
358 observed in surface seawater, especially at St. 25, where surface <sup>137</sup>Cs levels exceeded the  
359 global fallout values by about three orders of magnitude.

360 Distribution of <sup>137</sup>Cs in the water column of the western North Pacific Ocean was  
361 investigated in the framework of the WOMARS (Worldwide Marine Radioactivity Studies)  
362 project, carried out by IAEA during 1995-2005 (Livingston and Povinec, 2005; IAEA, 2005;  
363 Povinec et al., 2005b, 2010). On the basis of the data stored in the GLOMARD/MARIS  
364 database (Povinec et al. 2004b, 2005b, 2006; [www.iaea.org/monaco](http://www.iaea.org/monaco)), and taking into account  
365 an effective half-life of <sup>137</sup>Cs in surface waters of 13±1 yr (Povinec et al., 2005b), the  
366 background (global fallout) <sup>137</sup>Cs level for the western North Pacific Ocean was estimated to  
367 be (1.1 ± 0.1) mBq L<sup>-1</sup>. Unfortunately the IAEA'97 station (Fig. 1b) is not in the KoK region  
368 (called the Mixed-Water Region or Transition Zone), but it was under influence of the  
369 Kuroshio Current (Povinec et al., 2003). However, as we do not have better pre-Fukushima  
370 <sup>137</sup>Cs profiles we compare in Fig. 2b the KoK profiles with the IAEA'97 (St. 1, decay  
371 corrected to June 2011) profile. All KoK <sup>137</sup>Cs data are well above the IAEA'97 data,  
372 confirming thus Fukushima impact on all visited stations.

373 Fig. 2b compares the  $^{137}\text{Cs}$  water profiles with other post-Fukushima data (Ramzaev et al.  
 374 2014; Kumamoto et al., 2014, 2015; Aoyama et al. 2015a), which were measured in the  
 375 Transition Zone, however, some of the stations were outside of the KoK region. The highest  
 376  $^{137}\text{Cs}$  levels were measured at the KoK stations (St. 25 and 23) as well as at the UM and KT  
 377 stations situated closest to the coast. The surface  $^{137}\text{Cs}$  levels in the KoK region are mostly  
 378 between 0.1 and 1 Bq L<sup>-1</sup>, while the levels at other stations are below 0.1 Bq L<sup>-1</sup>. Although the  
 379 P10 stations (e.g. St. P10-098) are at larger distances from the coast than the RGS stations  
 380 (e.g. St. 7), their  $^{137}\text{Cs}$  levels are higher, indicating possible deposition of  $^{137}\text{Cs}$  from  
 381 radioactive clouds.

382 The inventory of a radionuclide in a seawater column was calculated by interpolating the  
 383 radionuclide concentration measured at each depth using the following equation

$$384 \quad I_R = \frac{1}{2} \left\{ \sum_{i=1}^N (W_{i+1} + W_i)(d_{i+1} - d_i) + 2W_1d_1 + 2W_N(d_B - d_N) \right\}, \quad (\text{eq. 3})$$

385 where  $I_R$  is the inventory of the radionuclide  $R$  in the seawater column (Bq/m<sup>2</sup>),  $N$  is the  
 386 number of sampling depths,  $W_i$  is the radionuclide concentration in seawater at depth  $i$ ,  $d_i$  is  
 387 the  $i$ -th sampling depth of seawater, and  $d_B$  is the total water depth to the bottom. For example  
 388 the  $^{137}\text{Cs}$  inventory calculated for the water column at St. 26 was  $(30 \pm 3)$  kBq m<sup>2</sup>. The total  
 389 inventories were calculated by integrating water column inventories and multiplying them by  
 390 the corresponding areas.

391 Our preliminary  $^{137}\text{Cs}$  inventory calculated for the KoK region was  $(2.2 \pm 0.3)$  PBq  
 392 (Povinec et al., 2013d), in reasonable agreement with previous estimation of Buessler et al.  
 393 (2012). In the present paper we included all the available  $^{137}\text{Cs}$  data measured during 2011-  
 394 2012 in the region (Honda et al., 2012; Kaeriyama et al., 2013; Kameník et al., 2013;  
 395 Ramzaev et al., 2014; Kumamoto et al., 2013a, 2014, 2015; Aoyama et al., 2016a, b), and we  
 396 got for the total inventory a value of  $(2.7 \pm 0.4)$  PBq. This lower value when compared with  
 397 the recent estimation of the direct liquid release inventory of  $(3.6 \pm 0.7)$  PBq (Aoyama et al.,  
 398 2015b), may be due to the fact that the investigated region covered only a limited area, 36 -  
 399 39°N and 141.5° - 148°E, as well as that part of the direct liquid discharges have already been  
 400 transported out of the investigated region when seawater sampling in 2011-2012 was carried  
 401 out.

402 Unfortunately we do not know a pre-Fukushima  $^{137}\text{Cs}$  inventory for the investigated  
 403 region. We may expect, however, that it will be lower than for the western North Pacific due  
 404 to the presence of Oyashio Intrusion waters in the western part of the Transition Zone (Tatebe

405 and Yasuda, 2004; Fig. 1a). Upwelling of deeper waters (with lower radionuclide levels)  
406 occurs in the Oyashio region, which are then transported by the Oyashio Intrusion to the  
407 western part of the Transition Zone, causing there a dilution of radionuclide levels (including  
408  $^{137}\text{Cs}$ ). Our estimation is that the pre-Fukushima  $^{137}\text{Cs}$  inventory in the western part of the  
409 KoK region should be around  $200 \text{ Bq m}^{-2}$  (for the top 200 m of the water column), i.e. by  
410 about a factor of two lower than the value estimated for the open western North Pacific Ocean  
411 (Aoyama and Hirose, 2004; Povinec et al. 2010). This global fallout background is negligible  
412 ( $\sim 0.01 \text{ PBq}$ ) when compared with the Fukushima impact on the  $^{137}\text{Cs}$  inventory in western  
413 North Pacific waters.

414

#### 415 4.2. Tritium

416

417 Tritium levels measured in the KoK samples varied in the range of 0.4-1.3 TU (Table 1), with  
418 the maximum at St. 25 (sampled at 10 m water depth) situated 30 km off the Fukushima coast  
419 (the closest station to the Fukushima NPP, Fig. 1a), where the radiocesium levels were also at  
420 their maxima (Table 1). All KoK sampling stations were affected by the Fukushima-derived  
421 tritium, the lowest tritium activity ( $0.37 \pm 0.02 \text{ TU}$ ) was found at St. 11 at 100 m water depth.  
422 As we already mentioned in the radiocesium section, the western KoK stations were under the  
423 influence of the Oyashio Intrusion, which should also dilute tritium concentrations in this  
424 region (Figs. 1a and 3).

425 The tritium seawater profiles (Fig. 3) generally follow the  $^{137}\text{Cs}$  water profiles presented in  
426 Fig. 2a. The average  $^3\text{H}/^{137}\text{Cs}$  activity ratio is  $0.5 \pm 0.3$  (Table 1), with high values at the  
427 depth of 100 m at St. 20, 26 and 25 (2.2, 2.0 and 1.2, respectively), indicating a penetration of  
428 tritium into deeper layers of the water column. On the other hand, the lowest  $^3\text{H}/^{137}\text{Cs}$  activity  
429 ratios (0.1-0.3) observed in surface waters (7-20 m) at several stations (e.g., St. 18, 27, 29, 30,  
430 31, 32) have been confirming the dominance of radiocesium in surface waters. Generally, the  
431 observed lower tritium than radiocesium levels may be attributed to lower tritium releases  
432 during the Fukushima accident, due to much lower fission yield of  $^3\text{H}$  compared to  $^{137}\text{Cs}$ , as  
433 well as due to the fact that the boiling water reactors produce much less tritium than the  
434 pressurized water reactors.

435 Although the most comprehensive oceanographic study with the most extensive coverage  
436 of  $^3\text{H}$  in the World Ocean was the WOCE (World Ocean Circulation Experiment,  
437 [www.eWOCE.org](http://www.eWOCE.org)) program conducted in the 1980s and 1990s, there were no sampling  
438 stations in the KoK region, which could be compared with our data. Tritium distribution in

439 the western North Pacific Ocean was also investigated in the framework of the WOMARS  
440 project. The background tritium level for the western North Pacific Ocean can be estimated  
441 from the GLOMARD/MARIS database (Povinec et al., 2004b, 2005b) to be  $(0.4 \pm 0.1)$  TU  
442 (decay corrected to June 2011).

443 The only available pre-Fukushima tritium profile in the KoK region is from Watanabe et  
444 al. (1991), measured in 1988 (Fig. 3, decay corrected to June 2011). Their results are  
445 generally lower when compared with the IAEA'97 station (Povinec et al., 2010), although the  
446  $^3\text{H}$  profiles should be between the GEOSECS (Ostlund et al., 1987) and the IAEA'97 profiles.  
447 This may be due to the fact that the Watanabe et al. (1991) station was located in the western  
448 Transition Zone (with influence of the Oyashio Intrusion), while the GEOSECS and IAEA  
449 stations were in the Subtropical Zone and in the Kuroshio region, respectively (Fig. 1b).  
450 Following the Watanabe et al. (1991) profile (Fig. 3), the pre-Fukushima tritium background  
451 concentration in surface water of the western KoK region can be as low as 0.2 TU, increasing  
452 thus the Fukushima impact on tritium levels by about a factor of six.

453 There was generally agreement between the GEOSECS, IAEA and Watanabe et al.  
454 stations regarding the vertical transport of tritium in the water column. A penetration of global  
455 fallout  $^3\text{H}$  down to about 1000 m depth has been observed, which also predicts the future  
456 transport of Fukushima tritium in the water column. The future penetration of Fukushima-  
457 derived tritium from surface waters into deeper layers of the ocean will be useful for studying  
458 pathways and time scales of deep-water formation (e.g. Povinec et al., 2010, 2011).

459 The tritium inventory in the water column at St. 26, situated close to the Fukushima coast,  
460 calculated using eq. 3 and the water depth profile data is  $(17 \pm 2)$  kBq  $\text{m}^2$ , which is  
461 approximately half of the  $^{137}\text{Cs}$  inventory in the same location, thus leading to the  $^3\text{H}/^{137}\text{Cs}$   
462 activity ratio of  $\sim 0.5$ . A preliminary estimation of the total  $^3\text{H}$  releases to the marine  
463 environment was in the range of 0.1-0.5 PBq (Povinec et al., 2013d). From the full set of  
464  $^3\text{H}/^{137}\text{Cs}$  activity ratios in the water column, and the previously estimated  $^{137}\text{Cs}$  releases to the  
465 sea, we may estimate the total  $^3\text{H}$  activity released and deposited offshore of the Fukushima  
466 coast to be  $(0.3 \pm 2)$  PBq.

467 Matsumoto et al. (2013) estimated the  $^3\text{H}$  concentration in the air during an early stage of  
468 the accident in March 2011 to be around 1.5 kBq  $\text{m}^3$ . The  $^3\text{H}$  levels in precipitation collected  
469 at distances 170-220 km from the Fukushima NPP during 21-23 March 2011 were up to 19  
470 Bq  $\text{L}^{-1}$  of water, about 27 times above the pre-Fukushima levels (Matsumoto et al. 2013), but  
471 still by a factor of 5 below the EU limit for  $^3\text{H}$  concentration in drinking water. Similarly, Liu  
472 et al. (2013) observed in Taiwan rains during May-December 2011  $^3\text{H}$  levels below 7 Bq  $\text{L}^{-1}$



473 of water. All these levels have been much lower than the tritium maximum (up to 1180 Bq L<sup>-1</sup>  
474 of water) observed in 1963 in the Northern Hemisphere precipitation after the large-scale  
475 atmospheric nuclear bomb tests carried out during 1961 and 1962 (Povinec et al., 2013a).

476 Measured tritium concentrations and the calculated tritium inventories confirm that the  
477 distribution of <sup>3</sup>H in the western North Pacific Ocean was influenced by the Fukushima  
478 accident. The pre-Fukushima tritium data, e.g. those previously gathered in the framework of  
479 the WOCE and WOMARS projects do not represent anymore global fallout distribution of  
480 this radionuclide in the western North Pacific Ocean.

481481

#### 482 4.3. Radiocarbon

483483

484 The observed <sup>14</sup>C levels in KoK water profiles (Fig. 4) show typical features: the  
485 concentrations were highest usually at the sub-surface layers (around -20‰ at 100-200 m  
486 water depth), and then they decreased down to around -115‰ at 400-500 m water depth. All  
487  $\Delta^{14}\text{C}$  values observed offshore Fukushima were negative, much lower when compared with  
488 the IAEA'97 (Aramaki et al., 2001; Povinec et al., 2004c), GEOSEC (Stuiver and Östlund,  
489 1983) and WOCE stations (Key et al. 1996, 2002, 2004). The <sup>14</sup>C of global fallout origin  
490 observed at these stations penetrated down to about 1000 m (Stuiver and Ostlund, 1983;  
491 Povinec et al., 2004c), similarly as it was observed in the case of <sup>3</sup>H (Ostlund et al., 1987;  
492 Povinec et al., 2010). The observed decrease in surface  $\Delta^{14}\text{C}$  levels after GEOSECS (~150‰  
493 in 1973; Stuiver and Östlund, 1983) and IAEA'97 (~90‰ in 1997; Povinec et al., 2004c)  
494 would predict  $\Delta^{14}\text{C}$  levels in 2011 around 50‰. However, all the measured  $\Delta^{14}\text{C}$  levels in  
495 2011 in the KoK samples were below 0‰, indicating that a comparison with IAEA and  
496 GEOSECS stations has not been appropriate because of different position of sampling  
497 stations. We have already noticed that <sup>3</sup>H levels in the western KoK region were influenced  
498 by Oyashio Intrusion, which brought low tritium activity waters to this region. In the case of  
499 <sup>14</sup>C the situation could be similar as the negative  $\Delta^{14}\text{C}$  values were observed at all visited  
500 stations, including water profiles at St. 11 and 20 down to 500 m water depth (Fig. 4). Pre-  
501 Fukushima <sup>14</sup>C water profiles, measured in the western North Pacific by Tsunogai et al.  
502 (1995) and Kumamoto et al. (2002) also showed negative  $\Delta^{14}\text{C}$  values (Fig. 4), however,  
503 these stations were located in the Oyashio region (Fig. 1b).

504 Surface <sup>14</sup>C concentration in seawater is regulated mainly by the CO<sub>2</sub> air – sea exchange,  
505 and the residence time of surface water in the region (Kumamoto et al., 2013b). Because of

506 the upwelling of deeper waters with lower  $^{14}\text{C}$  levels in the Oyashio region, and their  
507 transport by the Oyashio Intrusion to the western part of the Transition zone, the surface  $^{14}\text{C}$   
508 levels in this region are lower than in the Kuroshio region as a mixing of Oyashio and  
509 Kuroshio waters occur in the Transition Zone (Kumamoto et al., 2002). All KoK  $^{14}\text{C}$  stations  
510 located in the western Transition Zone showed negative  $\Delta^{14}\text{C}$  values, indicating that these  
511 stations were under the influence of the Oyashio Intrusion waters. On the other hand, St. C22  
512 and C23 sampled in 1993 by Aramaki et al. (2005) showed positive  $\Delta^{14}\text{C}$  values (around  
513 70‰), confirming that these stations were outside of the Oyashio Intrusion region (Fig. 1a, b).

514 The data presented in Fig. 4 show that the  $^{14}\text{C}$  levels measured in the KoK seawater  
515 samples are higher than the pre-Fukushima results measured in the Oyashio region (44°00'N,  
516 155°00'E) in 1997 by Kumamoto et al. (2002), but comparable with the results of Tsunogai et  
517 al. (1995) measured in 1985, also in the Oyashio region (43°00'N, 150°14'E). As we do not  
518 have pre-Fukushima  $^{14}\text{C}$  data for the KoK region, we may accept the Kumamoto et al. (2002)  
519 surface  $^{14}\text{C}$  data as a possible background for the KoK stations (after appropriate residence  
520 time corrections between 1997 and 2011). This assumption seems to be reasonable for surface  
521 St. 19, 21, 25 and 29 (the average  $\Delta^{14}\text{C}$  value being -55‰), however, the water profiles at  
522 St. 11 and 20 showed at 100 m and 200 m water depths increased  $\Delta^{14}\text{C}$  values to -20‰, while  
523 at water depths of 400 m and 500 m they decreased to around -115‰. If we take these deeper  
524 values as a possible background (as at the 400-500 m water depth we do not expect a  
525 Fukushima impact already in June 2011), the Fukushima contributions to  $^{14}\text{C}$  levels in the  
526 investigated region can be 6% and 9% for surface and 100-200 m water depths, respectively.  
527 As the KoK  $^{14}\text{C}$  stations were not located close to the coast, we may expect (similarly as in  
528 the case of  $^{137}\text{Cs}$  and  $^3\text{H}$ ) that the Fukushima impact on the  $^{14}\text{C}$  levels in the western part of  
529 the transition Zone could be even stronger.

530 There are no additional data available on radiocarbon levels in the atmosphere or in  
531 seawater after the Fukushima accident. Possible  $^{14}\text{C}$  contributions of Fukushima origin were  
532 discussed in tree rings of the Japanese cedar grown in Iwaki (Fukushima Prefecture, Xu et al.,  
533 2015), and in ginkgo leaf samples from Korea (Park et al., 2013). Both samples showed for  
534 2011 a smaller than expected decrease in  $^{14}\text{C}$  from the exponential trend, which may imply a  
535  $^{14}\text{C}$  release during the Fukushima accident.

536536

## 537 5. Conclusions

538538

539 The analysis of  $^{137}\text{Cs}$ ,  $^3\text{H}$  and  $^{14}\text{C}$  in surface and water column samples collected in the  
540 western North Pacific Ocean after the Fukushima accident showed that the Fukushima impact  
541 has been mainly on  $^{137}\text{Cs}$  in the marine environment. The  $^{137}\text{Cs}$  concentrations observed in  
542 surface seawater of the western North Pacific Ocean were due to the Fukushima accident  
543 higher by about three orders of magnitude. On the other hand the  $^3\text{H}$  levels were above the  
544 global fallout background only by about a factor of 6. The  $^{14}\text{C}$  data suggest that the impact on  
545 radiocarbon levels in the western North Pacific Ocean was measurable, but only around 9%  
546 above the background. The water column data indicated that the Fukushima-derived  
547 radionuclides already in June 2011 reached depths down to around 200 m.

548 The  $^{137}\text{Cs}$  inventory in the water column of the investigated western North Pacific Ocean  
549 affected by the Fukushima accident was estimated to be  $(2.7 \pm 0.4)$  PBq, which can be  
550 regarded as a lower limit of the direct  $^{137}\text{Cs}$  liquid discharges to the ocean. This lower value  
551 when compared with the recent estimation of the direct liquid release inventory of  $(3.6 \pm 0.7)$   
552 PBq (Aoyama et al., 2016b) may be due to the fact that the region under study did not cover  
553 the full area affected by the Fukushima liquid releases. On the basis of  $^3\text{H}/^{137}\text{Cs}$  activity ratios  
554 in the water column profiles, the total  $^3\text{H}$  inventory was estimated to be  $(0.3 \pm 0.2)$  PBq.

555 Measured tritium and radiocarbon concentrations in the western North Pacific Ocean  
556 confirm that their distribution has been influenced by the Fukushima accident. The pre-  
557 Fukushima tritium and radiocarbon data, e.g. those previously gathered in the framework of  
558 the WOCE and WOMARS projects, do not represent anymore the global fallout distribution  
559 of these radionuclide in the western North Pacific Ocean.

560 Further studies of these radionuclides in the water column of the North Pacific Ocean are  
561 necessary for better estimation of the atmospheric input (via a wet and dry deposition) to their  
562 total inventory. The investigated radionuclides will be useful tracers during the next decades  
563 for studying pathways, ocean currents and time scales of deep and bottom water formation,  
564 for studying biogeochemical processes in the water column, circulation of water masses in the  
565 North Pacific Ocean, and transport of North Pacific waters to the South Pacific and the Indian  
566 Oceans.

567567

## 568 **Acknowledgments**

569 The authors are thankful to Dr. S. Sheppard (Chief Editor of JER) for useful comments,  
570 and to prof. K. Hirose and dr. Y. Kumamoto for recent radiocesium data for the western  
571 North Pacific Ocean. We also thank Dr. K. O. Buesseler for provision of seawater samples  
572 collected during the A/V Ka'imikai-o-Kanaloa (KoK) cruise in the western North Pacific

573 Ocean, the Gordon and Betty Moore Foundation, and the Chemical Oceanography Program  
574 of the US National Science Foundation for funding the KoK expedition. The Bratislava group  
575 acknowledges a support provided by the EU Research and Development Operational Program  
576 (funded by the ERDF, Project No. 26240220004). The International Atomic Energy Agency  
577 is grateful to the Government of the Principality of Monaco for support provided to its  
578 Environment Laboratories.

579

## 580 **References**

581

582 Aarkrog, A., Baxter, M.S., Bettencourt, A.O., Bojanowski, R., Bologna, A., Charmasson, S.,  
583 Cunha, I., Delfanti, R., Duran, E., Holm, E., Jeffree, R., Livingston, H.D.,  
584 Mahapanyawong, S., Nies, H., Osvath, I., Pingyu, L., Povinec, P.P., Sanchez, A., Smith,  
585 J.N., Swift, D., 1997. A comparison of doses from  $^{137}\text{Cs}$  and  $^{210}\text{Po}$  in marine food: A  
586 major international study. *J. Environ. Radioact.* 34, 69–90.

587 Aoyama, M., Hirose, K., 2004. Artificial radionuclides database in the Pacific Ocean:  
588 HAM database. *ScientificWorldJournal* 4:200–215.

589 Aoyama, M., Tsumune, D., Hamajima, Y., 2012a. Distribution of  $^{137}\text{Cs}$  and  $^{134}\text{Cs}$  in the North  
590 Pacific Ocean: impacts of the TEPCO Fukushima-Daiichi NPP accident. *J. Radioanal.*  
591 *Nucl. Chem.* 296, 535–539.

592 Aoyama, M., Tsumune, D., Uematsu, M., Kondo, F., Hamajima, Y., 2012b. Temporal  
593 variation of  $^{134}\text{Cs}$  and  $^{137}\text{Cs}$  activities in surface water at stations along the coastline near  
594 the Fukushima Dai-ichi Nuclear Power Plant accident site, Japan. *Geochem. J.* 46, 321–  
595 325.

596 Aoyama, M., Uematsu, M., Tsumune, D., Hamajima, Y., 2013. Surface pathway of  
597 radioactive plume of TEPCO Fukushima NPP1 released  $^{134}\text{Cs}$  And  $^{137}\text{Cs}$ .  
598 *Biogeosciences*, 10, 3067–3078.

599 Aoyama, M., Hamajima, Y., Hult, M., Uematsu, M., 2016a.  $^{134}\text{Cs}$  and  $^{137}\text{Cs}$  in the North  
600 Pacific Ocean derived from the March 2011 TEPCO Fukushima Dai-ichi Nuclear Power  
601 Plant accident, Japan. Part one: surface pathway and vertical distributions. *J.*  
602 *Oceanography* 72, 53-65.

603 Aoyama, M., Kajino, M., Tanaka, T.Y., Sekiyama, T.T., Tsumune, D., Tsubono, T.,  
604 Hamajima, Y., Inomata, Y., Gamo, T., 2016b.  $^{134}\text{Cs}$  and  $^{137}\text{Cs}$  in the North Pacific Ocean  
605 derived from the TEPCO Fukushima Dai-ichi Nuclear Power Plant accident, Japan in  
606 March 2011: Part Two – Estimation of  $^{134}\text{Cs}$  and  $^{137}\text{Cs}$  inventories in the North Pacific  
607 Ocean. *J. Oceanography* 72, 67-76.

608 Aramaki, T., Mizushima, T., Kuji, T., Povinec, P.P., Togawa, O., 2001. Distribution of  
609 radiocarbon in the southwestern North Pacific. *Radiocarbon* 43, 857-867.

610 Aramaki, T., Togawa, O., Watanabe, S., Tsunogai, S., Taira, K., 2005. Temporal change of  
611 radiocarbon in the Western North Pacific. *JAERI Report*, Mutsu.

612 Buesseler, K.O., Jayne, S.R., Fisher, N.S., Rypina, I.I., Baumann, H., Baumann, Z., Breier, C.  
613 F., Douglass, E.M., George, J., Macdonald, A.M., Miyamoto, H., Nishikawa, J., Pike, S.

614 M., Yoshida, S., 2012. Fukushima-derived radionuclides in the ocean and biota off Japan.  
615 Proc. Nat. Acad. Sci. USA 109, 5984–5988.

616 Buzinny, M., Likhtarev, I., Los, I., Talerko, N., Tsigankov, N., 1998. <sup>14</sup>C analysis of annual  
617 tree rings from the vicinity of the Chernobyl NPP. Radiocarbon 40, 373–379.

618 Chino, M., Nakayama, H., Nagai, H., Terada, H., Katata, G., Yamazawa, H., 2011.  
619 Preliminary estimation of release amounts of <sup>131</sup>I and <sup>137</sup>Cs accidentally discharged from  
620 the Fukushima Daiichi nuclear power plant into the atmosphere. J. Nucl. Sci. Technol.,  
621 48, 1129–1134.

622 Chudý M., Povinec P., 1982. Radiocarbon production in CO<sub>2</sub> coolant of nuclear reactor.  
623 Acta Physica Univ. Comen. 22, 127-131.

624 Dietze, H., Kriest, I. 2012. <sup>137</sup>Cs off Fukushima Dai-ichi, Japan: model based estimates of  
625 dilution and fate. Ocean Sci. 8, 319-332.

626 Estournel, C., Bosc, E., Bocquet, M., Ulses, C., Marsaleix, P., Winiarek, V., Osvath, I.,  
627 Nguyen, C., Duhaut, T., Lyard, F., Michaud, H., Auclair, F., 2012. Assessment of the  
628 amount of Cesium-137 released into the Pacific Ocean after the Fukushima accident and  
629 analysis of its dispersion in Japanese coastal waters. J. Geophys. Res. 117, C11014. 630  
<http://dx.doi.org/10.1029/2012JC007933>.

631 Hernández-Ceballos, M.A., Hong, G.H., Lozano, R.L., Kim, Y.I., Lee, H.M., Kim, S.H., Yeh,  
632 S.W., Bolívar, J.P., Baskaran, M., 2012. Tracking the complete revolution of surface  
633 westerlies over Northern Hemisphere using radionuclides emitted from Fukushima, Sci.  
634 Total Environ. 438, 80-85.

635 Hirose, K., 2012. 2011 Fukushima Dai-ichi nuclear power plant accident: summary of  
636 regional radioactive deposition monitoring results. J. Environ. Radioact. 111, 13-17.

637 Honda, M., Aono, T., Aoyama, M., Hamajima, Y., Kawakami, H., Kitamura, M., Masumoto,  
638 Y., Miyazawa, Y., Takigawa, M., Saino, T., 2012 Dispersion of artificial caesium-134  
639 and -137 in the Western North Pacific one month after the Fukushima accident.  
640 Geochim. J. 46, 1–9.

641 Hou, X.L., Povinec, P.P., Zhang, L. Y., Biddulph, D., Chang, C.-C., Fan, Y.K., Golser, R.,  
642 Jeřkovský, M., Jull, A.J.T., Liu, Q., Shi, K. L., Steier, P., Zhou, W.J., 2013. Iodine-129 in  
643 seawater offshore Fukushima: Distribution, speciation, sources, and budget. Environ. Sci.  
644 Technol. 47, 3091-3098.

645 IAEA, 2005. Worldwide marine radioactivity studies (WOMARS). Radionuclide levels in  
646 oceans and sea. IAEA-TECDOC-1429, Vienna, Austria.

647 Inoue, M., Kofuji, H., Nagao, S., Yamamoto, M., Hamajima, Y., Yoshida, K., Fujimoto, K.,  
648 Takada, T., Isoda, Y., 2012, Lateral variation of <sup>134</sup>Cs and <sup>137</sup>Cs concentrations in surface  
649 seawater in and around the Japan Sea after the Fukushima Dai-ichi Nuclear Power Plant  
650 accident. J. Environ. Radioact. 109, 45-51.

651 Jean-Baptiste, P., Fourré, E., Dapigny, A., Baumier, D., Baglan, N., Alanic, G., 2010. <sup>3</sup>He  
652 mass spectrometry of very low-level measurement of organic tritium in environment  
653 samples J. Environ. Radioact. 101, 185–189.

654 Kaeriyama, H., Ambe, D., Shimizu, Y., Fujimoto, K., Ono, T., Yonezaki, S., Kato, Y.,  
655 Matsunaga, H., Minami, H., Nakatsuka, S., Watanabe, T. Direct observation of <sup>134</sup>Cs and

656  $^{137}\text{Cs}$  in surface seawater in the western and central North Pacific after the Fukushima Dai-  
657 ichi nuclear power plant accident (2013) *Biogeosciences*, 10 (6), pp. 4287-4295.

658 Kameník, J., Dulaiova, H., Buesseler, K.O., Pike S.M., Šťastná, K., 2013. Cesium-134  
659 and 137 activities in the central North Pacific Ocean after the Fukushima Dai-ichi 660  
Nuclear Power Plant accident. *Biogeosciences* 10, 6045–6052.

661 Kawamura, H., Kobayashi, T., Furuno, A., In, T., Ishikawa, Y., Nakayama, T., Shima, S.,  
662 Awaji, T., 2011. Preliminary numerical experiments on oceanic dispersion  $^{131}\text{I}$  and  $^{137}\text{Cs}$   
663 discharged into the ocean because of the Fukushima Dai-ichi nuclear power plant  
664 disaster. *J. Nucl. Sci. Technol.* 48, 1349–1356.

665 Key, R., Quay, P., Jones, G., McNichol, A., von Reden, K., Schneider, R., 1996. WOCE  
666 AMS radiocarbon I: Pacific Ocean results (P6, P16 and P17). *Radiocarbon* 38, 425-518.

667 Key, R., Quay, P., Schlosser, P., McNichol, A., von Reden, K., Schneider, R., Elder, K.,  
668 Stuiver, M., Ostlund, H., 2002. WOCE radiocarbon IV: Pacific Ocean results; P10,  
669 P13N, P14C, P18, P19 & S4P. *Radiocarbon* 44, 239-392.

670 Key, R.M., Kozyr, A., Sabine, C.L., Lee, K., Wanninkhof, R., Bullister, J.L., Feely, R.A.,  
671 Millero, F.J., Mordy, C., Peng, T.-H., 2004. A global ocean carbon climatology: Results  
672 from Global Data Analysis Project (GLODAP). *Global Biogeochem. Cy.* 18(4), GB4031.  
673 <http://dx.doi.org/10.1029/2004GB002247>.

674 Kim, H.G., Kong, T.Y., Lee, G.J., Jeong, W.T., Kim, S.T., 2011. Analysis of metabolism and  
675 effective half-life for radiation workers' tritium intake at pressurized heavy water  
676 reactors. *Progress Nucl. Sci. Technol.* 1, 545-548.

677 Kirchner, G., Bossew, P., De Cort, M., 2012. Radioactivity from Fukushima Dai-ich in air  
678 over Europe; part 2: what can it tell us about the accident? *J. Environ. Radioact.* 114, 35-  
679 40. <http://dx.doi.org/10.1016/j.jenvrad.2011.12.016>.

680 Kumamoto, Y., Murata, A., Saito, C., Honda, M., Kusakabe, M., 2002. Bomb radiocarbon  
681 invasion into the northwestern North Pacific. *Deep Sea Res. II* 49, 5339–5351.

682 Kumamoto, Y., Murata, A., Kawano, T., Aoyama, M., 2013a. Fukushima-derived  
683 radiocesium in the northwestern Pacific Ocean in February 2012. *Appl. Radiat. Isotopes*  
684 81, 335–339.

685 Kumamoto, Y., Murata, A., Kawano, T., Watanabe, S., Fukasawa, M., 2013b. Decadal  
686 changes in bomb-produced radiocarbon in the Pacific Ocean from the 1990s to 2000s.  
687 *Radiocarbon* 55, 1641–1650.

688 Kumamoto, Y., Aoyama, M., Hamajima, Y., Aono, T., Kouketsu, S., Murata, A., Kawano, T.,  
689 2014. Southward spreading of the Fukushima-derived radiocesium across the Kuroshio  
690 Extension in the North Pacific. *Sci. Rep.* 4, 4276. <http://dx.doi.org/10.1038/srep04276>.

691 Kumamoto, Y., Aoyama, M., Hamajima, Y., Murata, A., Kawano, T., 2015. Impact of  
692 Fukushima-derived radiocesium in the western North Pacific Ocean about ten months  
693 after the Fukushima Dai-ichi nuclear power plant accident. *J. Environ. Radioact.* 140,  
694 114-122.

695 Livingston, H.D., Povinec, P.P., 2000. Anthropogenic marine radioactivity. *Ocean and*  
696 *Coastal Management* 43, 689-712.

697 Livingston, H.D., Povinec, P.P., 2002. A millennium perspective on the contribution of global  
698 fallout radionuclides to ocean science. *Health Phys.* 82, 656-668.

699 Masson, O., Baeza, A., Bieringer, J., Brudecki, K., Bucci, S., Cappai, M., Carvalho, F.P.,  
700 Connan, O., Cosma, C., Dalheimer, A. Didier, D., Depuydt, G., De Geer, L.E., De  
Vismes, A., Gini, L., Groppi, F., Gudnason, K., Gurriaran, R., Hainz, D., Halldorsson, O.,  
702 Hammond, D., Hanley, O. Holey, K. Homoki, Zs., Ioannidou, A. , Isajenko, K.,  
703 Jankovick M., Katzlberger, C., Kettunen, M., Kierepko, R., Kontro, R. Kwakman, P.J.M.,  
704 Lecomte, M. , Leon Vintro, L. Leppänen, A.- P., Lind, B. , Lujaniene, G., Mc Ginnity, P.,  
705 Mc Mahon, C., Mala H., Manenti, S., Manolopoulou, M., Mattila, A., Mairing, A.,  
706 Mietelski, J.W., Møller, B.S., Nielsen, P., Nikolick J., Overwater, R.M.W., Palsson, S. E.,  
707 Papastefanou, C., Penev, I., Pham, M.K., Povinec, P.P., Ramebäck, H., Reis, M.C. ,  
708 Ringer, W., Rodriguez, A., Rulík, P., Saey, P.R.J. , Samsonov, V., Schlosser, C., Sgorbati,  
709 G. , Silobritiene, B. V., Söderström, C., Sogni, R., Solier, L., Sonck, M., Steinhauser, G.,  
710 Steinkopff, T. , Steinmann, P., Stoulos, S., Sykora, I., Todorovic, D., Tooloutalaie, N.,  
711 Tositti, L., Tschiersch, J., Ugron, A., Vagena, E., Vargas, A., Wershofen, H., Zhukova O.,  
712 2011. Tracking of airborne radionuclides from the damaged Fukushima Dai-Ichi nuclear  
713 reactors by European networks. *Environ. Sci. Technol.* 45, 7670-7677.

714 Matsumoto, T., Maruoka, T., Shimoda, G., Obata, H., Kagi, H., Suzuki, K.; Yamamoto, K.,  
715 Mitsuguchi, T., Hagino, K., Tomioka, N., Sambandam, C., Brummer, D., Klaus, P.M.,  
716 Aggarwal, P., 2013. Tritium in Japanese precipitation following the March 2011  
717 Fukushima Daiichi nuclear plant accident. *Sci. Total Environ.* 445-446, 365-370.

718 Miyazawa, Y., Masumoto, Y., Varlamov, S. M., Miyama, T., 2012a. Transport simulation of  
719 the radionuclide from the shelf to open ocean around Fukushima. *Continental Shelf Res.*  
720 50-51, 16-29.

721 Molnár, M., Hajdas, I., Janovics, R., Rinyu, L., Synal, H., Veres, M., Wacker, L., 2013a. C-14  
722 analysis of groundwater down to the milliliter level. *Nucl. Instrum. Meth. Phys. Res. B*  
723 294, 573-576.

724 Molnár, M., Janovics, R., Major, I., Orsovszki, J., Gönczi, R., Veres, M., Leonard, A.G.,  
725 Castle, S.M., Lange, T.E., Wacker, L., Hajdas, I., Jull, A.J.T., 2013b. Status report of the  
726 new AMS 14C sample preparation lab of the Hertelendi Laboratory of Environmental  
727 Studies (Debrecen, Hungary). *Radiocarbon* 55, 665-676.

728 Morino, Y., Ohara, T., and Nishizawa, M., 2011. Atmospheric behavior, deposition, and  
729 budget of radioactive materials from the Fukushima Daiichi nuclear power plant in  
730 March 2011. *Geophys. Res. Lett.* 38, L00G11. <http://dx.doi.org/10.1029/2011GL048689>.

731 Nakano, M., Povinec, P.P., 2003. Oceanic general circulation model for the assessment of the  
732 distribution of <sup>137</sup>Cs in the world ocean. *Deep-sea Res. II* 50, 2803-2816.

733 Nakano, M., Povinec, P.P., 2012. Long-term simulations of the <sup>137</sup>Cs dispersion from the  
734 Fukushima accident in the world ocean. *J. Environ. Radioact.* 111, 109-115.

735 Nishihara, K., Yamagishi, I., Yasuda, K., Ishimori, K., Tanaka, K., Kuno, T., Inada, S.,  
736 Gotoh, Y., 2012. Radionuclide release to stagnant water in Fukushima-1 Nuclear Power  
737 Plant. *Transactions of the Atomic Energy Society of Japan* 11, 13–19.

738 Ostlund, G.H., Craig, H., Broecker, W.B., Spencer, D., 1987. *GEOSECS Atlantic, Pacific and*  
739 *Indian ocean expeditions, vol.7, Shorebased data and graphics*, National Science  
740 Foundation, Washington, D.C., 200 pp.

741 Palcsu, L., Major, Z., Köllő, Z., Papp, L., 2010. Using an ultrapure  $^4\text{He}$  spike in tritium  
742 measurements of environmental water samples by the  $^3\text{He}$ -ingrowth method. *Rapid*  
743 *Comm. Mass Spectr.* 24, 698-704.

744 Park, J.H., Hong, W. Park, G. Sung, K.S., Lee, K.H., Kim, Y.E., Kim, J.K., Choi, H.W., Kim,  
745 G.D., Woo, H.J., Nakanishi, T., 2013. A comparison of distribution maps of  $\Delta^{14}\text{C}$  in  
746 2010 and 2011 in Korea. *Radiocarbon* 55, 841-847.

747 Pham, M. K., Betti, M., Povinec, P. P., Alifimov, V., Biddulph, D., Gastaud, J., Kieser, W. E.,  
748 Lopez Gutierrez J. M., Possnert, G., Sanchez-Cabeza, J. A., Suzuki, T., 2010. Certified  
749 reference material IAEA-418:  $^{129}\text{I}$  in Mediterranean Sea water. *J. Radioanal. Nucl. Chem.*  
750 286, 121–127.

751 Pham, M.K., Betti, M., Povinec, P.P., Benmansour, M., Bünger, V., Drefvelin, J., Engeler, C.,  
752 Flemal, J.M., Gasco, C., Guillevic, J., Gurriaran, R., Groening, M., Happel, J.D.,  
753 Herrmann, J., Klemola, S., Kloster, M., Kanisch, G., Leonard, K., Long, S., Nielsen, S.,  
754 Oh, J.-S., Rieth, P.U., Östergren, I., Pettersson, H., Pinhao, N., Pujol, L., Sato, K.,  
755 Schikowski, J., Varga, Z., Vartti, V.P., Zheng, J., 2011. A certified reference material for  
756 radionuclides in the water sample from Irish Sea (IAEA-443). *J. Radioanal. Nucl. Chem.*  
757 288, 603–611.

758 Povinec, P., Chudý, M., Sýkora, I., Szarka, J., Pikna, M., Holý, K., 1988. Aerosol  
759 radioactivity monitoring in Bratislava following the Chernobyl accident. *J. Radioanal.*  
760 *Nucl. Chem. Lett.* 126, 467-478.

761 Povinec, P.P., Oregioni, B., Jull, A.J.T., Kieser, W.E., Zhao, X.-L., 2000. AMS measurements  
762 of  $^{14}\text{C}$  and  $^{129}\text{I}$  in seawater around radioactive waste dump sites. *Nucl. Instrum. Methods*  
763 *Phys. Res. B* 172, 672-678.

764 Povinec, P.P., Badie, C., Baeza, A., Barci-Funel, G., Bergan, T.D., Bojanowski, R., Burnett,  
765 W., Eikenberg, J., Fifield, L.K., Serradell, V., Gastaud, J., Goroncy, I., Herrmann, J.,  
766 Hotchkis, M.A.C., Ikaheimonen, T.K., Jakobson, E., Kalimbadjan, J., La Rosa, J.J., Lee,  
767 S.-H., Liong Wee Kwong, L., Lueng, W.M., Nielsen, S.P., Nouredine, A., Pham, M.K.,  
768 Rohou, J.-N., Sanchez-Cabeza, J.A., Suomela, J., Suplinska, M., Wyse, E., 2002.  
769 Certified reference material for radionuclides in seawater IAEA-381 (Irish Sea water). *J.*  
770 *Radioanal. Nucl. Chem.* 251, 369-374.

771 Povinec, P.P., Livingston, H.D., Shima, S., Aoyama, M., Gastaud, J., Goroncy, I., Hirose, K.,  
772 Huyhn-Ngoc, L., Ikeuchi, Y., Ito, T., La Rosa, J., Liong Wee Kwong, L., Lee, S.-H.,  
773 Moriya H., Mulsow, S., Oregioni, B., Pettersson, H., Togawa, O., 2003. IAEA'97  
774 expedition to the NW Pacific Ocean – results of oceanographic and radionuclide  
775 investigations of the water column. *Deep-Sea Res. II* 50, 2607-2638.

776 Povinec, P.P., 2004a. Developments in analytical technologies for marine radioactivity  
777 studies. In: H.D. Livingston (Ed.) *Marine Radioactivity*. Elsevier, Amsterdam, 237-294.

778 Povinec, P.P., Comanducci, J.F., Levy-Palomo, I., 2004b. IAEA-MEL's underground  
779 counting laboratory in Monaco – background characteristics of HPGe detectors with anti-  
780 cosmic shielding. *Appl. Rad. Isotopes* 61, 85-93.

781 Povinec, P.P., K. Hirose, T. Honda, T. Ito, E.M. Scott, Togawa, O., 2004b. Spatial  
782 distribution of  $^3\text{H}$ ,  $^{90}\text{Sr}$ ,  $^{137}\text{Cs}$  and  $^{239,240}\text{Pu}$  in surface waters of the Pacific and Indian  
783 Oceans – GLOMARD database. *J. Environ. Radioact.* 76, 113-137.



784 Povinec, P.P., Aramaki, T., Burr, G.S., Jull, A.J.T., Liong Wee Kwong, L., Togawa, O.,  
785 2004c. Radiocarbon in the water column of the southwestern North Pacific Ocean – 24  
786 years after GEOSECS. *Radiocarbon* 46, 583-594.

787 Povinec, P.P., Comanducci, J.F., Levy-Palomo, I., 2005a. IAEA-MEL's underground  
788 counting laboratory (CAVE) for the analysis of radionuclides in the environment at very  
789 low-levels. *J. Radioanal. Nucl. Chem.* 263, 441-445.

790 Povinec, P. P., Aarkrog, A., Buesseler, K.O., Delfanti, R., Hirose, K., Hong, G.H., Ito, T.,  
791 Livingston, H.D., Nies, H., Noshkin, V.E., Shima, S., Togawa, O., 2005b. <sup>90</sup>Sr, <sup>137</sup>Cs and  
792 <sup>239,240</sup>Pu concentration surface water time series in the Pacific and Indian Oceans –  
793 WOMARS results. *J. Environ. Radioact.* 81, 63-87.

794 Povinec, P.P., Scotto, P., Osvath, I., Ramadan, H. 2006. The Marine Information System  
795 (MARIS). In: *Isotopes in Environmental Studies*. IAEA, Vienna, 68–69.

796 Povinec, P. P., Lee, S. H., Liong Wee Kwong, L., Oregioni, B., Jull, A. J. T., Kieser, W. E.,  
797 Morgenstern, U., Top, Z., 2010. Tritium, radiocarbon, <sup>90</sup>Sr and <sup>129</sup>I in the Pacific and  
798 Indian Oceans. *Nucl. Instrum. Methods Phys. Res. B* 268, 1214-1218.

799 Povinec, P.P., Breier, R., Coppola, L., Groening, M., Jeandel, C., Jull, A.J.T., Kieser, W.E.,  
800 Top, Z., 2011. Tracing of water masses using a multi-isotope approach in the southern  
801 Indian Ocean. *Earth Planetary Sci. Lett.* 302, 14-26.

802 Povinec, P.P., Hirose, K., Aoyama, M., 2012a. Radiostrontium in the western North Pacific:  
803 Characteristics, behavior, and the Fukushima impact. *Environ. Sci. Technol.* 46, 10356-  
804 10363.

805 Povinec, P. P., Eriksson, M., Scholten, J., Betti, M., 2012b. Marine Radioactivity Analysis.  
806 In: M.F. L'Annunziata (Ed.) *Handbook on Radioactivity Analysis*. Academic Press,  
807 Amsterdam, 770-832.

808 Povinec, P.P., Hirose, K., Aoyama, M., 2013a. Fukushima Accident: Radioactivity Impact on  
809 the Environment. Elsevier, New York, 382 pp.

810 Povinec, P.P., Gera, M., Hirose, K., Lujaniené G., Nakano, M., Plastino, W., 2013b.  
811 Dispersion of Fukushima radionuclides in the global atmosphere and the ocean. *Appl.*  
812 *Rad. Isotopes* 81, 383–392.

813 Povinec, P.P., Sýkora, I., Gera, M., Holý, K., Brest'áková, L., Kováčik, A., 2013c.  
814 Fukushima-derived radionuclides in ground-level air of Central Europe: a comparison  
815 with simulated forward and backward trajectories. *J Radioanal Nucl Chem* 295, 1171–  
816 1176. <http://dx.doi.org/10.1007/s10967-012-1943-3>.

817 Povinec, P.P., Aoyama, M., Biddulph, D., Breier, R., Buesseler K., Chang, C.C., Golser, R.,  
818 Hou, X.L., Jeřkovský, M., Jull, A.J.T., Kaizer, J., Nakano, M., Nies, H., Palcsu, L., Papp,  
819 L., Pham, M.K., 10, Steier, P., Zhang, L.Y., 2013d. Cesium, iodine and tritium in NW  
820 Pacific waters – a comparison of the Fukushima impact with global fallout.  
821 *Biogeosciences* 10, 5481–5496.

822 Povinec, P.P., Ženišová, Z., Šivo, A., Ogrinc, N., Richtáriková, M., Breier, R., 2013e.  
823 Radiocarbon and stable isotopes as groundwater tracers in the Danube river basin of SW  
824 Slovakia. *Radiocarbon* 55, 1017-1028.

825 Povinec, P.P., Hirose, K., 2015. Fukushima radionuclides in the NW Pacific, and assessment  
826 of doses for Japanese and world population from ingestion of seafood. *Sci. Rep.* 5, 9016.  
827 <http://dx.doi.org/10.1038/srep09016>.

828 Ramzaev, V., Nikitin, A., Sevastyanov, A., Artemiev, G., Bruk, G., Ivanov, S., 2014.  
829 Shipboard determination of radiocesium in seawater after the Fukushima accident:  
830 Results from the 2011-2012 Russian expeditions to the Sea of Japan and western North  
831 Pacific Ocean. *J. Environ. Radioact.* 135, 13-24.

832 Rinyu, L., Molnár, M., Major, I., Nagy, T., Veres, M., Kimák, Á., Wacker, L., Synal, H.A.,  
833 2013. Optimization of sealed tube graphitization method for environmental C-14 studies  
834 using MICADAS. *Nucl. Instrum. Meth. Phys. Res. B* 294, 270-275.

835 Rypina, I.I., Jayne, S.R., Yoshida, S., Macdonald, A.M., Douglass, E., Buesseler, K., 2013.  
836 Short-term dispersal of Fukushima-derived radionuclides off Japan: modeling efforts and  
837 model-data intercomparison. *Biogeosciences* 10, 4973-4990.  
838 <http://dx.doi.org/10.5194/bg-10-4973-2013>, 2013.

839 Steinhauser, G., 2014. Fukushima's Forgotten Radionuclides: A Review of the Understudied  
840 Radioactive Emissions. *Environ. Sci. Technol.* 48, 4649-4663.

841 Stohl, A., Seibert, P., Wotawa, G., Arnold, D., Burkhardt, J. F., Eckhardt, S., Tapia, C.,  
842 Vargas, A., Yasunari, T. J., 2012. Xenon-133 and caesium-137 releases into the  
843 atmosphere from the Fukushima Dai-ichi nuclear power plant: determination of the  
844 source term, atmospheric dispersion, and deposition. *Atmos. Chem. Phys.* 12, 2313–  
845 2343.

846 Stuiver, M., Ostlund, H.G., 1983. GEOSECS Indian and Mediterranean radiocarbon.  
847 *Radiocarbon* 25, 1-29.

848 Schwantes, J.M., Orton, C.R., Clark, R.A., 2012. Analysis of a nuclear accident: fission and  
849 activation product releases from the Fukushima Daiichi Nuclear Facility as remote  
850 indicators of source identification, extent of release, and state of damaged spent nuclear  
851 fuel. *Environ. Sci. Technol.* 46, 8621-8627.

852 Tatebe, H., Yasuda, I., 2004. Oyashio Southward Intrusion and Cross-Gyre Transport Related  
853 to Diapycnal Upwelling in the Okhotsk Sea. *J. Phys. Oceanogr.* 34, 2327-2341.

854 Tsumune, D., Tsubono, T., Aoyama, M., Hirose, K., 2012. Distribution of oceanic <sup>137</sup>Cs from  
855 the Fukushima Dai-ichi Nuclear Power Plant simulated numerically by a regional ocean  
856 model. *J. Environ. Radioact.* 111, 100–108.

857 Tsumune, D., Tsubono, T., Aoyama, M., Uematsu, M., Misumi, K., Maeda, Y., Yoshida, Y.,  
858 Hayami, H., 2013. One-year, regional-scale simulation of <sup>137</sup>Cs radioactivity in the ocean  
859 following the Fukushima Daiichi Nuclear Power Plant accident. *Biogeosciences* 10,  
860 5601–5617.

861 Tsunogai, S., Watanabe, S., Honda, M., Aramaki, T., 1995. North Pacific Intermediate Water  
862 studied chiefly with radiocarbon. *J. Oceanogr.* 51, 519–536.

863 UNSCEAR, 2008. United Nations Scientific Committee on the Effects of Atomic Radiation:  
864 Sources and Effects of Ionizing Radiation. Report to the General Assembly. United  
865 Nations, New York, USA.

866 Watanabe, Y.W., Watanabe, S., Tsunogai, S., 1991. Tritium in the northwestern North  
867 Pacific. *Journal of the Oceanographical Society of Japan* 47 (3), 80-93.

868 Xu, S., Cook, G.T., Cresswell, A.J., Dunbar, E., Freeman, S.P.H.T., Hastie, H., Hou, X.,  
869 Jacobsson, P., Naysmith, P., Sanderson, D.C.W., 2015. Radiocarbon concentration in  
870 modern tree rings from Fukushima, Japan. *J. Environ. Radioact.* 146, 67-72.

871 Yoshida, N., Kanda, J., 2012. Tracking the Fukushima Radionuclides. Science 336, 1115-  
872 1116.  
873  
874

875

876 **Table 1**877 Tritium, radiocarbon and radiocesium in seawater samples collected offshore Fukushima during the  
878 KoK cruise.

879

Station number	Position of the sampling station	Water depth (m)	$^3\text{H}$ (TU)	$\Delta^{14}\text{C}$ (‰)	$^{134}\text{Cs}$ ( $\text{Bq L}^{-1}$ )	$^{137}\text{Cs}$ ( $\text{Bq L}^{-1}$ )	$^3\text{H}/^{137}\text{Cs}$
2	34°30' N, 147°00' E	100			0.029 ± 0.009	0.027 ± 0.009	
		200			0.016 ± 0.006	0.015 ± 0.006	
6	36°30' N, 147°00' E	20				0.026 ± 0.009	
8	37°30' N, 147°00' E	5	0.90 ± 0.06				
		20			0.178 ± 0.009	0.184 ± 0.010	
		50			0.160 ± 0.012	0.158 ± 0.014	
		100			0.059 ± 0.006	0.051 ± 0.007	
11	37°30' N, 144°00' E	20			0.085 ± 0.008	0.072 ± 0.009	
		50			0.105 ± 0.011	0.080 ± 0.009	
		100	0.37 ± 0.02	-19.5 ± 2.9	0.018 ± 0.009	0.037 ± 0.009	1.18 ± 0.03
		200		-10.4 ± 2.6			
		400		-89.9 ± 3.2			
18	37°00' N, 143°00' E	500		-113.4 ± 3.0			
		20	0.74 ± 0.055		0.234 ± 0.017	0.252 ± 0.021	0.35 ± 0.03
		50			0.426 ± 0.029	0.425 ± 0.031	
		100			0.048 ± 0.009	0.035 ± 0.009	
19	37°33' N, 142°57' E	5		-61.5 ± 3.0			
20	38°00' N, 143°00' E	20	1.05 ± 0.05		0.188 ± 0.014	0.171 ± 0.016	
		100					
		200	0.74 ± 0.05	-21.0 ± 3.5	0.023 ± 0.005	0.039 ± 0.009	2.24 ± 0.2
		400		-20.5 ± 3.0	0.015 ± 0.005	0.019 ± 0.007	
21	37°30' N, 142°30' E	500		-102.3 ± 3.5			
		5		-116.8 ± 2.9			
		20		-50.6 ± 3.1			
		50	0.96 ± 0.09		0.292 ± 0.027	0.135 ± 0.013	
		100			0.117 ± 0.011	0.135 ± 0.013	0.84 ± 0.08
22	38°00' N, 142°30' E	8			0.836 ± 0.052	0.841 ± 0.060	
		10			0.217 ± 0.016	0.203 ± 0.016	
		20			0.087 ± 0.009	0.083 ± 0.009	
		50	0.78 ± 0.09		0.122 ± 0.009	0.138 ± 0.010	0.67 ± 0.08
24	38°00' N, 142°00' E	100			0.053 ± 0.007	0.052 ± 0.008	
		8			0.064 ± 0.009	0.054 ± 0.007	
		50			0.215 ± 0.013	0.201 ± 0.014	
		75			0.091 ± 0.009	0.094 ± 0.009	
25	37°31' N, 141°27' E	130			0.023 ± 0.006	0.029 ± 0.005	
		5		-38.5 ± 3.2			
		10			0.968 ± 0.054	1.120 ± 0.065	
		20	1.28 ± 0.09		0.225 ± 0.018	0.221 ± 0.019	0.68 ± 0.07
		50				0.057 ± 0.012	
26	37°00' N, 141°24' E	90			0.083 ± 0.009	0.064 ± 0.009	
		100	0.96 ± 0.08		0.120 ± 0.036	0.091 ± 0.030	1.24 ± 0.1
		7	0.75 ± 0.06		0.453 ± 0.031	0.441 ± 0.034	0.20 ± 0.02
		20			0.368 ± 0.023	0.386 ± 0.026	
		50	0.68 ± 0.03		0.256 ± 0.012	0.241 ± 0.012	0.33 ± 0.02
		75	0.73 ± 0.02		0.167 ± 0.013	0.188 ± 0.015	0.46 ± 0.02
		90	0.62 ± 0.03		0.085 ± 0.009	0.086 ± 0.009	0.85 ± 0.04
100	1.22 ± 0.03		0.064 ± 0.006	0.072 ± 0.007	2.00 ± 0.06		

		125		0.028 ± 0.008	0.042 ± 0.008	
		173	0.76 ± 0.25			
27	36°30' N, 141°24' E	10	0.90 ± 0.09	0.741 ± 0.034	0.748 ± 0.038	0.14 ± 0.02
28	36°01' N, 141°24' E	10	0.63 ± 0.06			
29	36°30' N, 142°05' E	0		-70.8 ± 3.4		
		10	0.79 ± 0.06	0.377 ± 0.016	0.438 ± 0.019	0.21 ± 0.02
30	36°30' N, 142°30' E	10	0.64 ± 0.02	0.765 ± 0.034	0.798 ± 0.040	0.095 ± 0.005
31	37°00' N, 142°30' E	10	0.70 ± 0.02	0.452 ± 0.023	0.480 ± 0.027	0.172 ± 0.007
		20		0.546 ± 0.027	0.555 ± 0.029	
		50		0.473 ± 0.022	0.481 ± 0.025	
32	37°00' N, 142°00' E	7	0.69 ± 0.10	0.287 ± 0.021	0.311 ± 0.022	0.26 ± 0.04

---

880

881

882

883

884

885

886

887

888

889

890

891

892

893

894

895

896

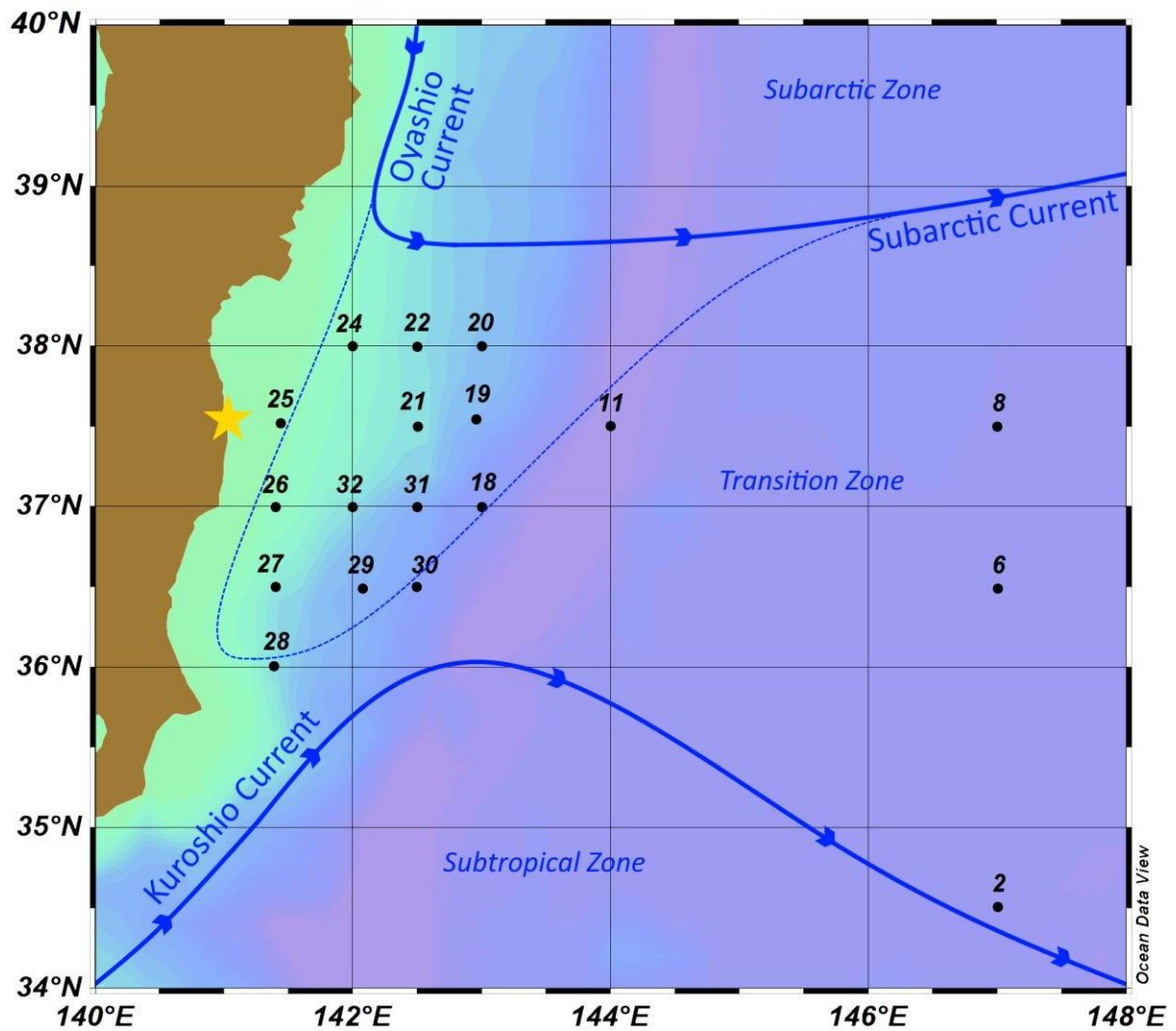
897

898

899

900

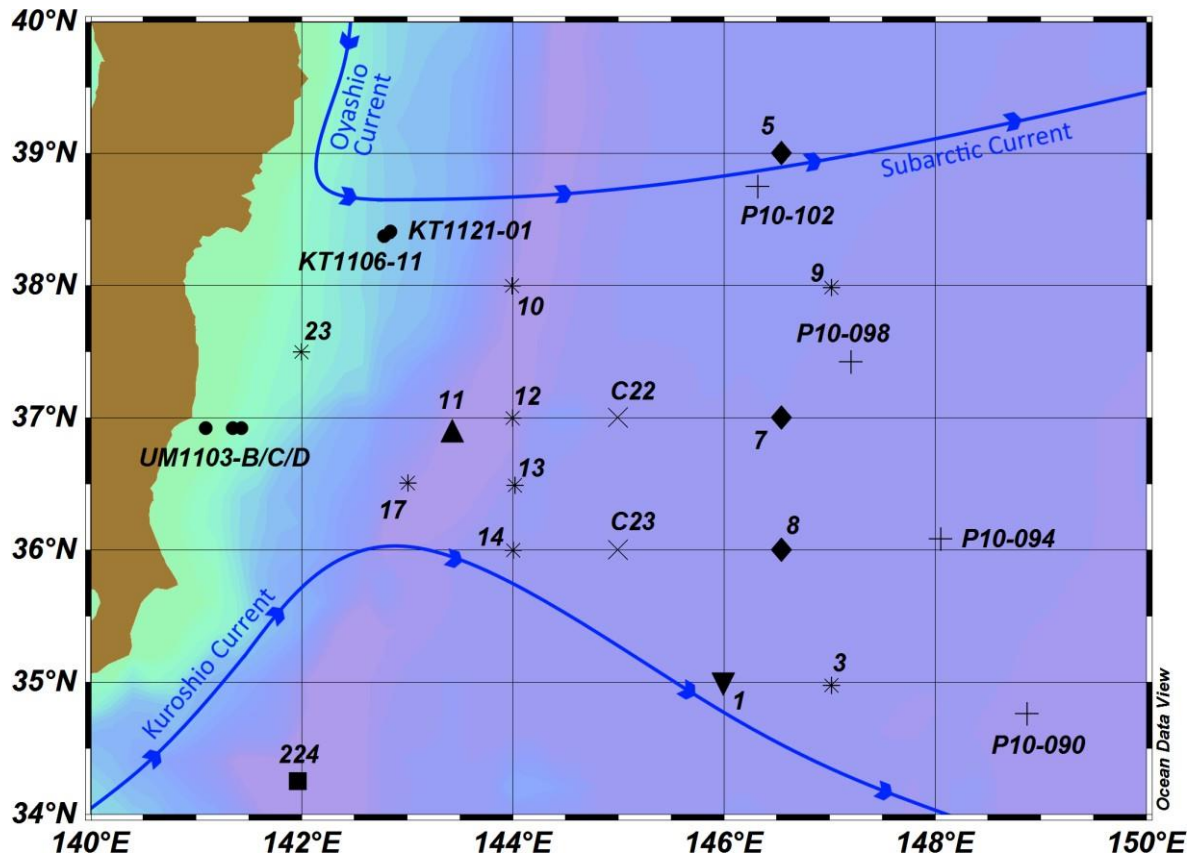
901



903

904 **Fig. 1a.** Locations of water sampling stations in the western North Pacific Ocean during the  
 905 KoK expedition used in this study. Fukushima Dai-ichi NPP accident location is indicated  
 906 with the star. Approximate positions of the Kuroshio and Oyashio Currents are shown as well.  
 907 The dashed line represents the southward intrusion of the Oyashio Current (Tatebe and  
 908 Yasuda, 2004).

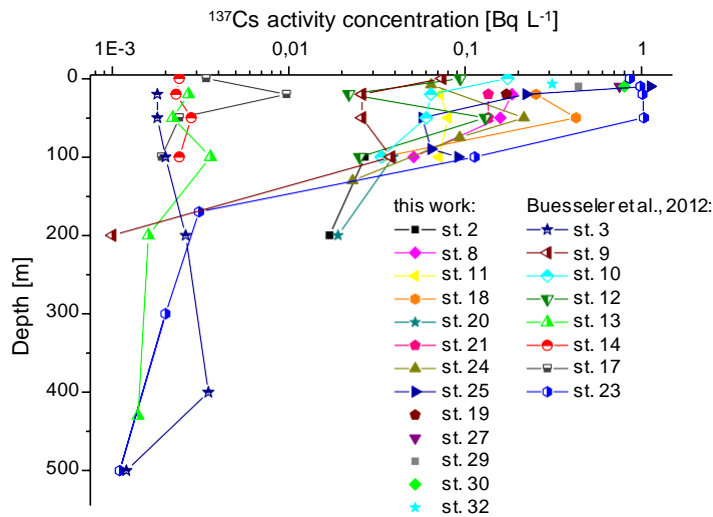
909



910

911 **Fig. 1b.** Locations of sampling stations used for data comparison: ● - UM11 and KT11  
 912 stations sampled for  $^{137}\text{Cs}$  in 2011 (Aoyama et al., 2016a); \* - selected KoK stations sampled  
 913 for  $^{137}\text{Cs}$  in June 2011 (Buesseler et al., 2012); × - KH93 stations sampled for  $^{14}\text{C}$  in 1993  
 914 (Aramaki et al., 2005); ■ - GEOSECS station sampled for  $^3\text{H}$  (Ostlund et al., 1987) and for  
 915  $^{14}\text{C}$  in 1973 (Stuiver and Ostlund, 1983); ▼ - IAEA '97 station sampled in 1997 for  $^{137}\text{Cs}$   
 916 (Povinec et al., 2003),  $^3\text{H}$  (Povinec et al., 2010) and  $^{14}\text{C}$  (Povinec et al., 2004c); + - P10-  
 917 stations sampled for  $^{137}\text{Cs}$  in 2012 (Kumamoto et al., 2015); ◆ - RGS stations sampled for  
 918  $^{137}\text{Cs}$  in 2012 (Ramzaev et al., 2014); ▲ - KH88 station sampled for  $^3\text{H}$  in 1988 (Watanabe et  
 919 al., 1991; The KH85 station sampled for  $^{14}\text{C}$  in 1985 (43° 00'N 150° 14' E; Tsunogai et al.,  
 920 1995), and the MR97 stations sampled for  $^{14}\text{C}$  in 1997 (44° 00'N, 155° 00' E; Kumamoto et al.,  
 921 2002) were situated outside of the KoK region.

922



923

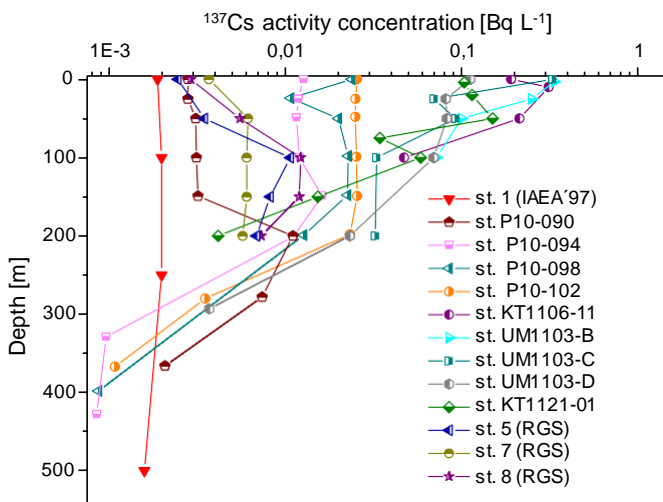
924 **Fig. 2a.**  $^{137}\text{Cs}$  activity concentration in seawater samples collected offshore Fukushima NPP  
 925 during the KoK cruise, compared with published data measured during the KoK cruise by  
 926 Buessler et al. (2012). For locations of the sampling stations see Figs. 1a, b.

927

928

929

930



931

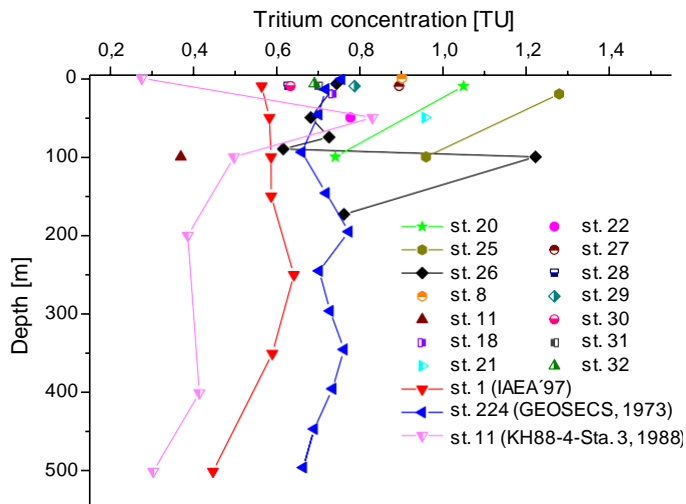
932

933 **Fig. 2b.**  $^{137}\text{Cs}$  activity concentration in seawater samples collected offshore Fukushima NPP  
 934 during the KoK cruise (decay corrected to June 2011), compared with published data  
 935 measured during the IAEA '97 cruise (Povinec et al., 2003), the RGS cruise (Ramzaev et al.,  
 936 2014), the P10 cruise (Kumamoto et al., 2015) and the UM11 and KT11 cruises (Aoyama et  
 937 al. (2016a). For locations of the sampling stations see Figure 1b.

938

939

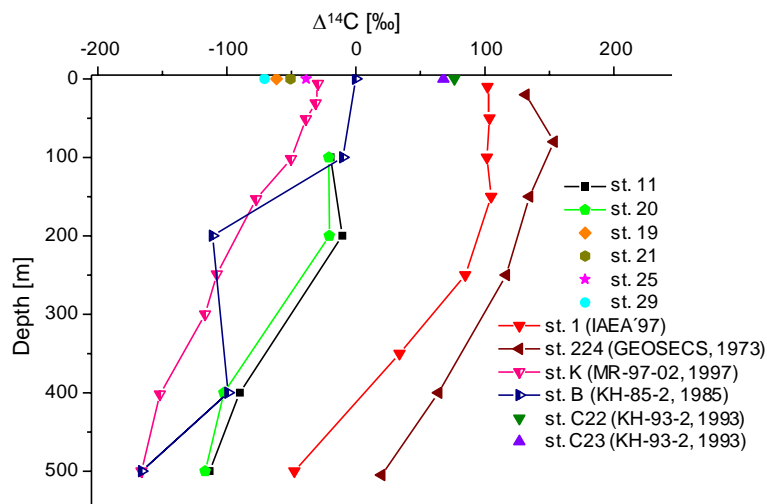




940

941 **Fig. 3.** Tritium concentration in seawater samples collected offshore Fukushima during the  
 942 KoK cruise (decay corrected to June 2011), compared with the results from the  
 943 GEOSECS (Ostlund et al., 1987), KH88 (Watanabe et al., 1991) and IAEA'97 (Povinec  
 944 et al., 2003) expeditions. For locations of the sampling stations see Figure 1b.  
 945

946



947

948

949 **Fig. 4.** Radiocarbon concentration in seawater samples collected offshore Fukushima during  
 950 the KoK cruise (decay corrected to June 2011), compared with the results from the  
 951 GEOSECS (Stuiver and Otlund, 1983), IAEA'97 (Povinec et al., 2004c), KH-85 (Tsunogai et  
 952 al., 1995), KH93 (Aramaki et al., 2005) and MR97 (Kumamoto et al., 2002) expeditions. For  
 953 locations of the sampling stations see Figure 1b.

954

955